Cell Reports
Medicine

Article

Ongoing evolution of SARS-CoV-2 drives escape from mRNA vaccine-induced humoral immunity

Graphical abstract

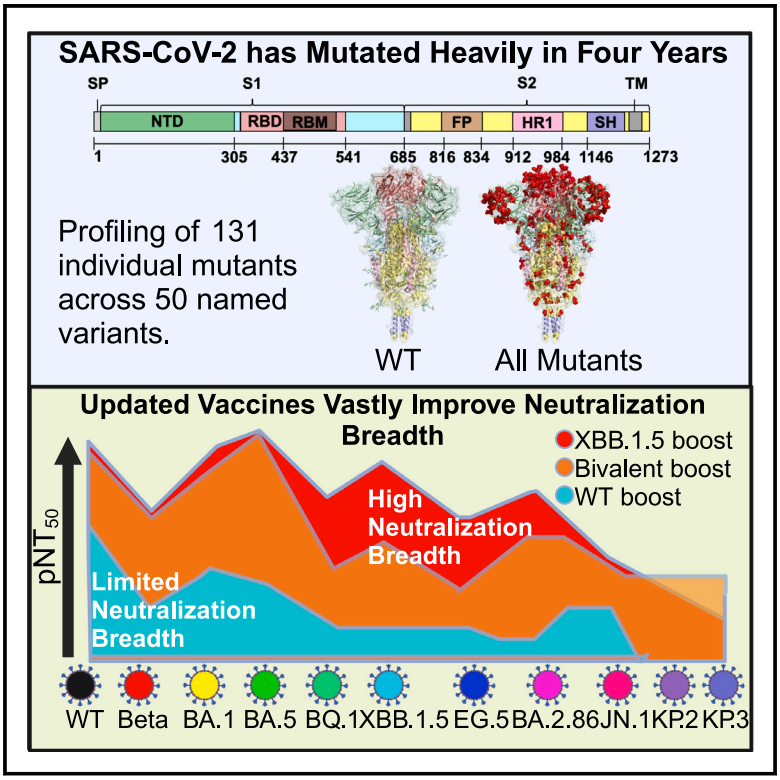

Highlights

- Primary vaccination reveals regions of vulnerability within the mutational landscape
- mRNA booster vaccination significantly enhances neutralization of SARS-CoV-2 mutants
- Individual omicron mutants reveal gaps in mRNA-boosted humoral immunity
- Variant-specific vaccines markedly improve neutralization breadth

Authors

Alex L. Roederer, Yi Cao, Kerri St. Denis, ..., Stefan Gravenstein, Wilfredo F. Garcia-Beltran, Alejandro B. Balazs

Correspondence

abalazs@mgh.harvard.edu

In brief

Roederer et al. examine how the SARS-CoV-2 virus evolves over time and how well updated vaccines protect against variants. Variants of the virus are becoming harder for vaccine-mediated humoral immunity to neutralize, even with updated boosters, suggesting alternate vaccination methods may be necessary to combat SARS-CoV-2 evolution.

Roederer et al., 2024, Cell Reports Medicine *5*, 101850
December 17, 2024
https://doi.org/10.1016/j.xcrm.2024.101850

CellPress

Cell Reports Medicine

CellPress
OPEN ACCESS

Article

Ongoing evolution of SARS-CoV-2 drives escape from mRNA vaccine-induced humoral immunity

Alex L. Roederer,[1] Yi Cao,[1] Kerri St. Denis,[1] Maegan L. Sheehan,[1] Chia Jung Li,[1] Evan C. Lam,[1] David J. Gregory,[2,3] Mark C. Poznansky,[2,4] A. John Iafrate,[5] David H. Canaday,[6,7] Stefan Gravenstein,[8,9,10] Wilfredo F. Garcia-Beltran,[1,5] and Alejandro B. Balazs[1,11,*]

[1]Ragon Institute of MGH, MIT, and Harvard, Cambridge, MA 02139, USA
[2]Vaccine and Immunotherapy Center, Massachusetts General Hospital, Boston, MA 02129, USA
[3]Pediatric Infectious Disease, Massachusetts General Hospital for Children, Boston, MA 02114, USA
[4]Massachusetts General Hospital Cancer Center, Boston, MA 02114, USA
[5]Department of Pathology, Massachusetts General Hospital, Boston, MA 02114, USA
[6]Case Western Reserve University School of Medicine, Cleveland, OH, USA
[7]Geriatric Research Education and Clinical Center, Louis Stokes Cleveland Department of Veterans Affairs Medical Center, Cleveland, OH, USA
[8]Center of Innovation in Long-Term Services and Supports, Veterans Administration Medical Center, Providence, RI, USA
[9]Division of Geriatrics and Palliative Medicine, Alpert Medical School of Brown University, Providence, RI, USA
[10]Brown University School of Public Health Center for Gerontology and Healthcare Research, Providence, RI, USA
[11]Lead contact
*Correspondence: abalazs@mgh.harvard.edu
https://doi.org/10.1016/j.xcrm.2024.101850

SUMMARY

With the onset of the COVID-19 pandemic 4 years ago, viral sequencing continues to document numerous individual mutations in the viral spike protein across many variants. To determine the ability of vaccine-mediated humoral immunity to combat continued SARS-CoV-2 evolution, we construct a comprehensive panel of pseudoviruses harboring each individual mutation spanning 4 years of the pandemic to understand the fitness cost and resistance benefits of each. These efforts identify numerous mutations that escape from vaccine-induced humoral immunity. Across 50 variants and 131 mutants we construct, we observe progressive loss of neutralization across variants, irrespective of vaccine doses, as well as increasing infectivity and ACE2 binding. Importantly, the recent XBB.1.5 booster significantly increases titers against most variants but not JN.1, KP.2, or KP.3. These findings demonstrate that variants continue to evade updated mRNA vaccines, highlighting the need for different approaches to control SARS-CoV-2 transmission.

INTRODUCTION

Since it was described in late 2019, SARS-CoV-2 has undergone continuous evolution. The virus originated in Wuhan, China, and was declared a global pandemic on March 11, 2020 by the World Health Organization (WHO).[1,2] Since then, it has infected over 700 million people and caused nearly 7 million deaths.[2,3] The first mutation to become fixed in the population, D614G, emerged in February of 2020 and was shown to be more infectious and stable than the original sequence.[4,5] However, the first variant to be named, B.1.1.7 or Alpha, harbored multiple mutations and became the dominant strain in the UK, exhibiting over 50% greater infectivity than the wild type (WT).[6] As the pandemic entered its second year, additional variants emerged carrying mutations in the receptor-binding domain (RBD) that enhanced transmissibility[7,8] through improved ACE2 binding and exhibited viral escape from convalescent sera.[9–11] Numerous studies in the first two years of the pandemic reported mutations including L452R,[12,13] K417N/T,[6,14,15] E484K,[16] N501Y,[17] Q677H,[18,19] and P618H/R,[20,21] which exhibited immune evasiveness, stronger ACE2 binding, or increased fusogenicity and infectivity. In the subsequent two years, the number of variants that have been documented has increased significantly, with mutations (predominantly in the RBD) that enable escape from vaccine-induced neutralizing antibodies and enhance transmissibility.[10,22–25]

An unprecedented effort to develop effective countermeasures resulted in multiple vaccines being approved by the Food and Drug Administration (FDA) in the United States, all of which were based upon the WT SARS-CoV-2 spike protein containing stabilizing mutations that were previously identified for respiratory synctial virus (RSV) and Middle East respiratory syndrome (MERS).[26,27] Numerous vaccine technologies were employed, including mRNA containing lipid nanoparticles, recombinant proteins, or adenovirus-vectored vaccines[28–31]; however, mRNA vaccines were the most widely deployed in the United States. Clinical trials of these vaccines demonstrated remarkable efficacy to reduce COVID-19 infections, hospitalizations, and deaths.[28–31]

However, the emergence of the Omicron variant and declining antibody titers over time led to the recommendation of a third

booster dose of mRNA vaccine by the FDA, yielding neutralizing, cross-reactive antibodies against Omicron.[23,32] The emergence of variants such as BA.5 in 2022 necessitated the reformulation of vaccines,[33] spurring the transition from monovalent to bivalent vaccines incorporating both WT and BA.5 spikes.[34] Despite the efficacy of the original vaccines in preventing severe disease and death, their effectiveness waned against heavily mutated, highly transmissible variants such as BQ.1.1, XBB, BA.2.86, and their sub-variants.[25,35–37] These highly evolved strains carried 34–58 total mutations within the spike protein, with 28 of these mutations in the RBD in the more recent variant JN.1. Numerous studies have highlighted vaccine evasion by individual spike mutations found in these strains, namely V445P,[38,39] N460K,[40] and F486 P/S,[41–44] among others.[16,17,21,43,45–52] In the fall of 2023, an FDA advisory committee recommended deployment of an updated monovalent mRNA vaccine encoding the XBB.1.5 spike.[53] However, JN.1 and its derivatives KP.2 and KP.3 make up over 90% of COVID sequences being submitted to GISAID.[54,55] We find that the latest XBB.1.5 booster enhances neutralizing activity against many variants that escaped bivalently boosted sera; however, the latest JN.1 variant remains significantly resistant to neutralization across vaccinations.

To understand the impact of mutations that have arisen across the shifting vaccination landscape, we constructed a library of individual spike transgenes harboring each individual mutation found in variants of concern or interest. Using this resource, we conducted a comprehensive analysis of escape by individual mutations that emerged during the pandemic. Using a previously validated high-throughput assay,[10,23,56] we measured the neutralization of pseudoviruses representing each individual mutation across a cohort of study participants who had received either the primary vaccine series (two shots) or the booster series (three shots) and were COVID naive. Furthermore, we evaluated the neutralization activity of sera from boosted individuals against all individual mutations, as well as strains harboring combinations of mutations through JN.1, totaling 220 different pseudoviruses. In addition, we profiled recombinant ACE2 binding of all 220 spike expression constructs to assess differences across individual mutants and variants. Interestingly, we find that a handful of individual mutations arising enable significant escape from boosted serum but also have reduced ACE2 binding. Remarkably, more recent variants, including BQ.1.1, XBB, and XBB.1.5, exhibit escape from boosted sera that is comparable to SARS-CoV-1 and the related pre-emergent WIV1 strain. However, sera from individuals receiving bivalent and XBB.1.5 boosters exhibited significant neutralizing activity against all variants. Despite this, variants such as EG.5, HK.3, and JN.1 exhibit substantial escape from bivalent boosted sera while KP.2 and KP.3 significantly escape XBB.1.5 boosted sera, suggesting that SARS-CoV-2 remains ahead of efforts to update vaccines. Variants not only increased escape over time, but they also drastically increased their infectivity and ACE2 binding ability. Together, these results highlight the importance of continued surveillance of SARS-CoV-2 sequence evolution and support the updating of existing vaccines. At the same time, our results also demonstrate the need to develop approaches capable of inducing broadly neutralizing humoral immunity to counter the continued evolution of SARS-CoV-2.

RESULTS

Comprehensive neutralization assays with primary vaccine sera reveal regions of vulnerability within the natural mutation landscape

SARS-CoV-2 has resulted in over 700 million infections and nearly 7 million deaths since it emerged in 2020.[2,3] The virus, which originated in Wuhan, China, circulated for nearly a year before the variant of concern (Alpha) emerged (Figure 1A; Table S1); however, in subsequent years, numerous variants of concern and interest have been described (Figure 1B; Table S1). The mutations of each variant are highlighted on the structure of a full-length spike protein to indicate how many mutations on the WT structure each variant carries but are not meant to be the structures of the variants. One of the most globally dominant variants, Delta (B.1.617.2), was ascendant in June 2021 and harbored 8 mutations, including 2 in the RBD.[9,55] However, the Omicron variant (BA.1), containing 32 spike mutations, rapidly rose to prominence after it appeared in November 2021. Variants derived from BA.1 continued to emerge resulting in the BA.5 strain harboring two additional mutations within the RBD. JN.1 then became the dominant strain globally[55] and harbor 58 total spike mutations with 27 of these in the RBD.[54] Impressively, the SARS-CoV-2 pandemic has now resulted in variants that are further evolved (by number of mutations) from the original Wuhan strain than other distinct coronaviruses such as RaTG13[57,58] (Figure 1C), which harbors only 26 amino acid changes shown on the structure of the WT spike for reference. Over the course of the pandemic, 164 individual mutations in viral spike have arisen across variants of concern/interest up to JN.1, including several that occurred at the same position in the WT spike protein numbering (Figure 1D).

To investigate the effect of all individual spike variations on vaccine-induced humoral immunity, we studied a cohort of 20 COVID naive donors (as defined by nucleocapsid serum reactivity) who had received the primary vaccine series (Table S2). Sera from this group were subjected to pseudovirus-based neutralization assays that we and others have previously validated.[10,23,56,60–64] In brief, pseudotyped lentiviral particles bearing a given SARS-CoV-2 spike protein and encoding a luciferase-expressing transgene were produced and mixed with serially diluted donor serum before ACE2-expressing target cells were added (Figure 1E). Assays were performed using pseudoviruses representing 69 differences present across 24 named variants of concern/interest up to and including Delta (Figures 2A and S1A). Variants with multiple consensus sequences such as Beta (V1–V6) are denoted as separate variants (Figure S1A). Donor serum exhibited high neutralizing activity against the Wuhan pseudovirus, with a geometric mean pseudovirus 50% neutralization titer (pNT_{50}) of 2,962 (Figure S1B). However, individual changes in either the N-terminal domain (NTD), RBD, or other portions of the S1 region exhibited significant escape from neutralization (Figure 2B), many of which have been previously reported.[14–16,18–21,46,47,65,66] Mutations that significantly escaped sera from the primary vaccine were found to be enriched in specific regions within the RBD and NTD (Figure 2C). Recombinant ACE2 binding to spike at the cell surface was assessed to explore the impact of individual mutations on

CellPress
OPEN ACCESS

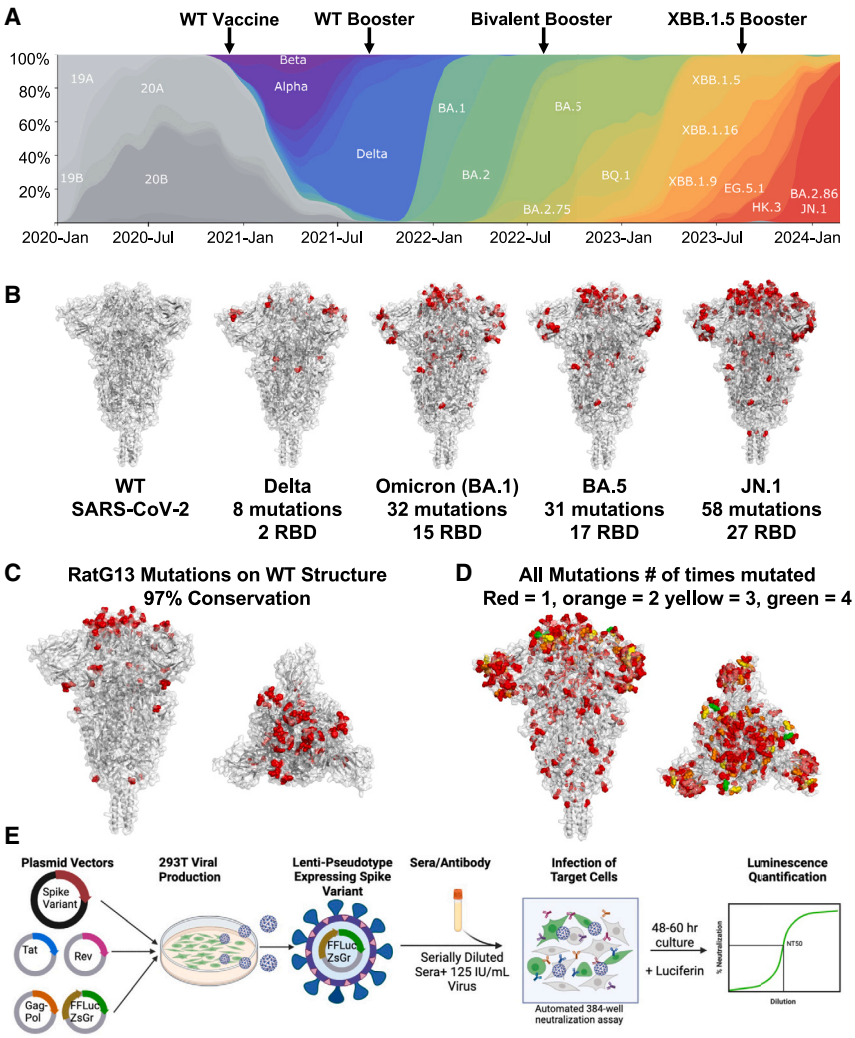

Figure 1. SARS-CoV-2 variants of concern harbor spike protein mutations that are enriched in the RBD

(A) Scaled stacked area chart of variants emerging during the SARS-CoV-2 pandemic. Arrows denote when each vaccine was made available. Adapted from nextstrain.org. Data as of February 28, 2024.

(B) Crystal structures of pre-fusion stabilized SARS-CoV-2 spike trimer (PDB ID 6XR8,[59] https://doi.org/10.2210/pdb6XR8/pdb) highlighting mutations found in each strain mapped onto their locations on the wild-type spike trimer. From left to right WT, Delta (B.1.617.2), Omicron (BA.1), BA.5, and JN.1 strains. Mutations highlighted for each strain are from corresponding Table S1.

(C) Crystal structure of pre-fusion stabilized SARS-CoV-2 spike trimer (PDB ID 6XR8,[59] https://doi.org/10.2210/pdb6XR8/pdb) with differences with the closely related RaTG13 coronavirus highlighted in red (front and top view) on the WT spike trimer.

(D) Crystal structure of pre-fusion stabilized SARS-CoV-2 spike trimer (PDB ID 6XR8,[59] https://doi.org/10.2210/pdb6XR8/pdb) with all 164 mutations found in variants of concern and variants of interest up to and including JN.1, mapped onto the WT spike, and colored by the number of times they have been observed in a single variant of concern or variant of interest. Red = 1, orange = 2 yellow = 3, green = 4.

(E) Schematic of high-throughput neutralization assay used in these studies.

ACE2 binding (Figure S1C). Many of the mutations that escaped the primary vaccine reduced ACE2 binding, suggesting a trade-off between viral escape and receptor binding, as was previously reported for K417N/T[14,15,65] (Figure 2D). Individual mutations rarely increased ACE2 binding; however, several including ΔH69V70, D215G, D614G, and H655Y achieved statistical significance (Figure S1C). To explore the interplay between resistance and ACE2 binding, we correlated neutralization resistance to ACE2 binding and found a significant correlation between stronger ACE2 binding and neutralization resistance (Figure 2E). Despite this, a majority of mutations (57 total, 82%) decreased ACE2 binding relative to WT suggesting that variants arose to escape immunity but not necessarily to improve receptor binding. Only 7 mutations both increased ACE2 binding and were harder to neutralize, most notably D614G, indicating that, at the individual mutation level, it is difficult for the virus to optimize for both parameters simultaneously. To explore individual vaccine responses, two-way hierarchical clustering was performed across all mutations tested for each individual donor (Figure 2F). This analysis revealed that sera from naive patients receiving the primary vaccine had remarkably similar losses of neutralizing activity across the subset of mutations illustrated in Figure 2B, with more than half of all mutations being harder to neutralize than WT. Interestingly, two separate clusters of donors were observed in this cohort, with the bottom cluster having a broader overall response to individual mutations arising through the Delta strain. However, we found no correlation across time, age, or gender to account for vaccination outcomes (not shown). These results suggest that humoral responses in most individuals were focused on particular epitopes within the NTD, RBD, and the rest of S1, following the primary vaccination regimen with approximately half of these individuals generating broader responses.

Combinations of individual RBD mutations yield neutralization resistance and impact ACE2 binding

Given that variants of concern/interest harbor multiple mutations, we assessed the impact of combinations of RBD mutations focusing on the Beta and Delta variants, which both readily escaped sera from primary vaccinees. We have previously shown that the RBD region of Beta was largely responsible for escape from neutralization.[10] To understand how multiple RBD mutations might coordinate to escape humoral immunity, primary vaccine sera were tested against double and triple RBD mutants (Figure 3A). Neither single mutation came close to recapitulating

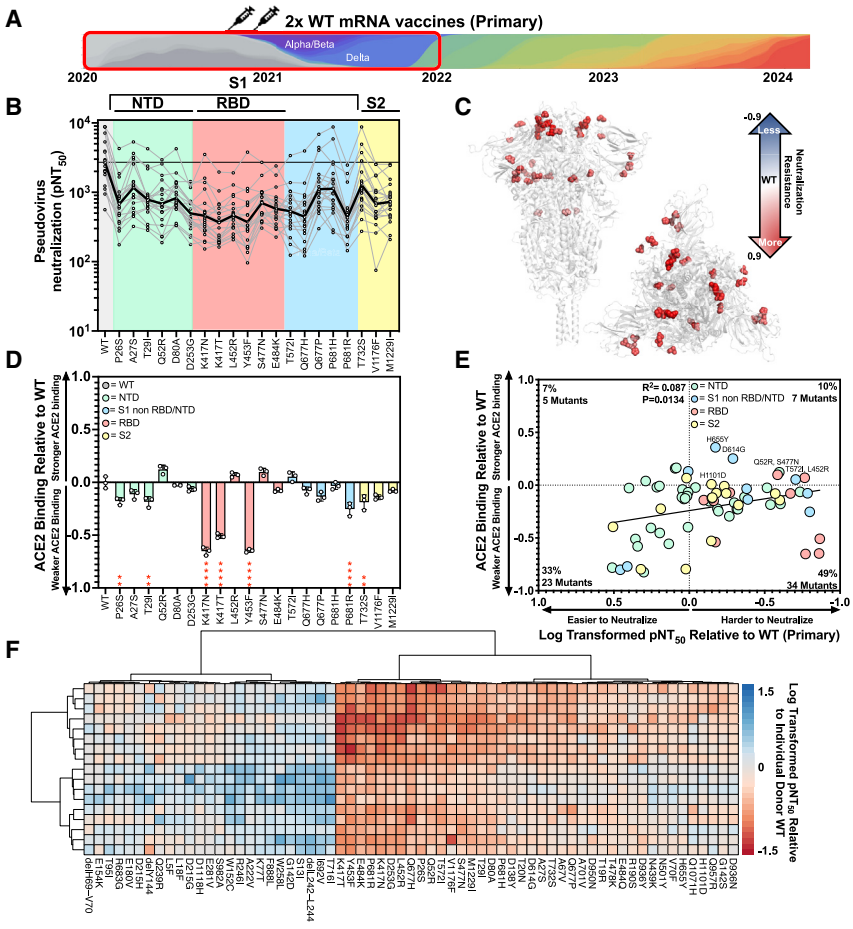

Figure 2. Comprehensive neutralization assays with primary vaccine sera revealed regions of vulnerability within the natural mutation landscape

(A) Schematic illustrating the time period from which variants were selected and the vaccinee sera to be tested below.

(B) Titers (n = 2 per sample per pseudovirus) that achieve 50% of pseudovirus neutralization (pNT_{50}) are plotted for mutants with significant escape primary vaccination regimen (2 doses of Pfizer) found in SARS-CoV-2 through Delta (1.617.2). The solid black line represents geometric mean pNT_{50} for reference. The following abbreviations are used: NTD, N-terminal domain; RBD, receptor binding domain; S1, S1 subunit; S2, S2 subunit.

(C) Spike structure (PDB ID: 6XR8,[59] https://doi.org/10.2210/pdb6XR8/pdb) with mutations critical for escape from primary vaccine sera mapped onto the spike. The geometric mean pNT_{50} value for mutations relative to WT was log transformed into a B factor on a scale of −0.9 to 0.9.

(D) Individual pseudovirus mutants that escaped primary vaccinees were measured for ACE2 binding. These values were then normalized to WT binding and log transformed. Binding was done for each mutant in technical triplicates (n = 3). Data are represented as mean ± SD ($*p < 0.0332$, $**p < 0.0021$, $***p < 0.0002$, $****p < 0.0001$).

(E) Neutralization titer relative to WT (average of n = 2) for primary vaccinees was plotted against ACE2 binding relative to WT (average of n = 3). Both values are log transformed, and a correlation between them was detected with p = 0.0134. Numbers of mutations and percentages in each quadrant are listed, and mutations are colored according to their location on the spike.

(F) Two-way hierarchical clustering of pNT_{50} values of sera obtained from vaccinated donors (rows) across each variant (columns) relative to individual donor WT titer. pNT_{50} values are plotted in a heatmap colored according to neutralizing activity relative to WT. Donors with WT neutralizing titers at the maximum of our assay were excluded. Mutations where a significant majority of donor titers reached the limit of detection were also excluded. Clustering was performed using pheatmap package v1.0.12 in RStudio.

the neutralization resistance of the parent spike, but we did observe an additive effect for the three individual RBD mutations found in the Beta variant. Combinations of any two mutations yielded greater resistance to neutralization than single mutations, but the triple mutant exhibited nearly as much escape as the full Beta spike. In contrast to Beta, combining RBD mutations in Delta resulted in no additional reduction in pNT_{50}, suggesting that mutations outside of RBD, likely P681R, which was highly resistant as well, appear to coordinate with L452R to drive greater escape (Figure 3B). To understand the impact that these combinations had on ACE2 binding, recombinant ACE2 staining was performed and binding relative to WT was assessed (Figures 3C and 3D). Of note, individual RBD mutations in Beta drastically reduced ACE2 binding, but combining all three significantly increased ACE2 binding (Figure 3C). In contrast, individual RBD mutations in the Delta variant exhibited modest changes in ACE2 binding; however, the combination of both exhibited significantly lower ACE2 binding than WT. Importantly, mutations outside of RBD restored ACE2-binding activity in the Delta variant, highlighting the importance of sequence context when evaluating individual mutations (Figure 3D).

mRNA booster vaccination significantly enhances neutralization of SARS-CoV-2 mutants

During a significant spike in COVID-19 cases in July 2021 stemming from the Delta variant, a third mRNA booster shot consisting of the same Wuhan spike formulation as the primary series was introduced in the United States[67] (Figure 4A). To measure the impact of a third mRNA administration on humoral immunity, 22 COVID-naive (by nucleocapsid test) samples from mRNA-boosted donors were subjected to neutralization assays across the same set of individual mutations reported through October 2021 (up to the Delta variant) (Figure S2A). Donors were age and WT pNT_{50} matched to the primary series donors (Table S3). The vast majority of mutants tested were more potently neutralized relative to the WT titer by serum from boosted donors than those who had only received the primary series (Figure S2B). Mutations that significantly escaped primary series were easier for boosted donors to neutralize, relative to WT titer (Figure 4B). However, 9 of these were still able to significantly escape boosted serum (Figure 4C), including P26S, Y453F, V1176F, and M1229I. Interestingly, some mutants, including D80A, K417N, T572I, and Q677H, exhibited

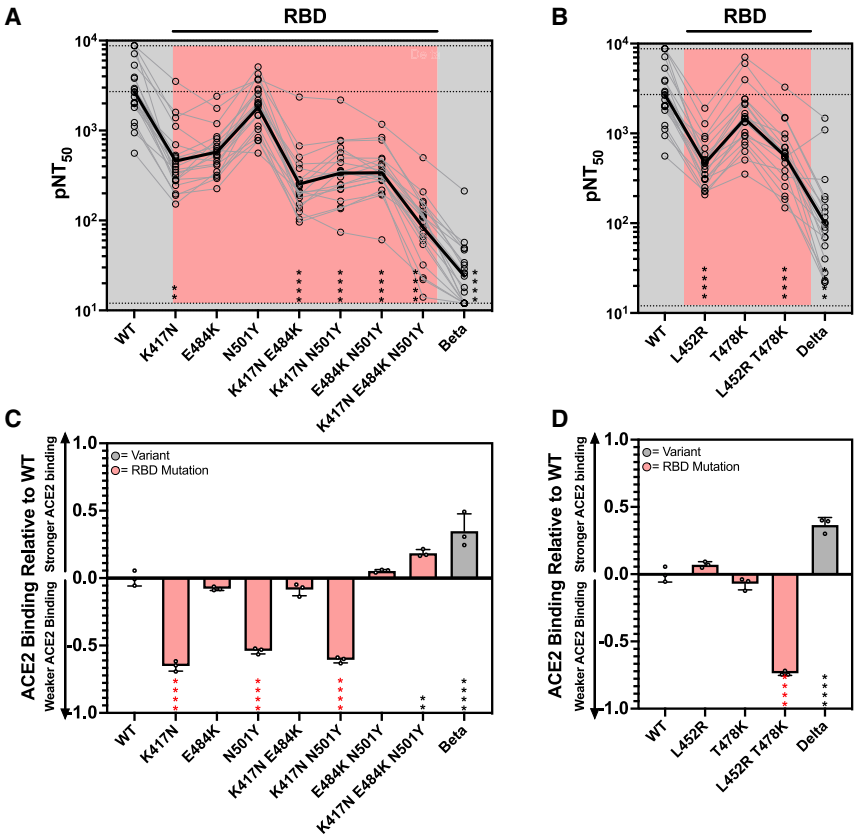

Figure 3. Combinations of individual mutations yield neutralization resistance and variable ACE2 binding

(A and B) Primary series vaccinee sera (average of $n = 2$) was tested via pseudovirus-based neutralization assays against combinations of RBD mutations found in the (A) Beta variant or (B) Delta strain. Each variant was compared to the wild type using a one-way ANOVA with Friedman's test and Dunn's multiple comparisons test. (* = $p < 0.0332$, ** = $p < 0.0021$, *** = $p < 0.0002$, **** = $p < 0.0001$).

(C and D) Single, double, or triple RBD mutants for the Beta (C) and Delta (D) variants were measured for ACE2 binding. Mutants were co-transfected with a zsgreen plasmid to be expressed on the surface of cells, and ACE2 binding was measured using a fluorescently labeled recombinant ACE2 protein using median fluorescence intensity of ACE2 Alexa 647, spike-positive (green) cells. Experiments were performed in technical triplicates ($n = 3$). Data are represented as mean ± SD. These values were then normalized to WT binding and log transformed. ACE2 binding was compared to WT using a one-way ANOVA with Dunn's multiple comparisons test. (*$p < 0.0332$, **$p < 0.0021$, ***$p < 0.0002$, ****$p < 0.0001$). *, significantly worse ACE2 binding.

disproportionately greater neutralization relative to WT, suggesting that these epitopes were preferentially targeted by booster vaccination (Figure 4D). However, boosting resulted in an overall broadening against nearly all individual mutations that had occurred through Delta (Figure 4D). Comparison between the two groups found that donors who received the booster vaccine had significantly increased neutralization activity overall (Figure 2E). Two-way hierarchical clustering was performed across all mutations tested for each individual donor (Figure S2C). Boosting greatly enhanced the breadth of neutralizing titers relative to WT for all but 1 of the 13 donors we analyzed (Figure S2C). Taken together, our results confirm previous reports that booster vaccination increases breadth against SARS-CoV-2 variants.[23,68–71]

Individual Omicron mutants reveal sites of resistance that are also found in more recent strains, against boosted sera

In November of 2021, a SARS-CoV-2 variant harboring an unusually large number of mutations was identified in South Africa.[72] This variant of concern, designated Omicron (BA.1), contained 59 mutations in its genome, 32 of which were in the spike protein, with 15 in the RBD. A number of heavily mutated, highly transmissible variants have descended from BA.1 since this time.[35,73,74] Neutralization assays were performed to assess whether boosted sera exhibited improved activity against 132 more recent mutations across 48 named variants (Figures S3A and 5A). While sera from individuals receiving a third mRNA booster vaccine were able to neutralize most mutants (Figure S3B), spike mutations V445P, N460K, and F486P exhibited the highest fold decrease in pNT_{50} (Figure 5B), which others have reported as critical for escape.[40–44,75] Notably, many other mutations significantly escaped boosted serum including V213E, insR214-EPE, G252V, G339D, G339H, L368I, and Y453F (Figure 5B). Despite their antibody escape, most of these mutations also exhibited reduced ACE2 binding when analyzed individually (Figure 5C). These results further support the concept of a trade-off between binding and escape with the exception of N460K, which was previously reported to increase both ACE2 binding and escape.[40] Across the full set of mutations arising since the beginning of the pandemic, numerous individual mutations escaped from mRNA-boosted serum samples (Figure S5B). Most of these also decreased ACE2 binding relative to WT, except for N460K, D614G, and H655Y, which significantly increased binding (Figure S3C). The relationship between ACE2 binding and boosted serum neutralization resistance was significantly correlated ($p = 0.0002$); however, 88% of mutants decreased ACE2 binding relative to WT (Figure 5D). This suggests that combinations of individual mutations were necessary to achieve both increased ACE2 binding and neutralization resistance. However, we identified 7 individual mutants that increased both ACE2 binding and escape, some of which had been previously reported including S477N,[76,77] L452R,[12,13] and D614G.[4,5,78]

As compared to mutations that emerged in variants up to and including Delta, those emerging from Omicron onwards exhibited significantly less neutralization by boosted sera ($p = 0.0021$) (Figure S4A). Interestingly, individual mutations

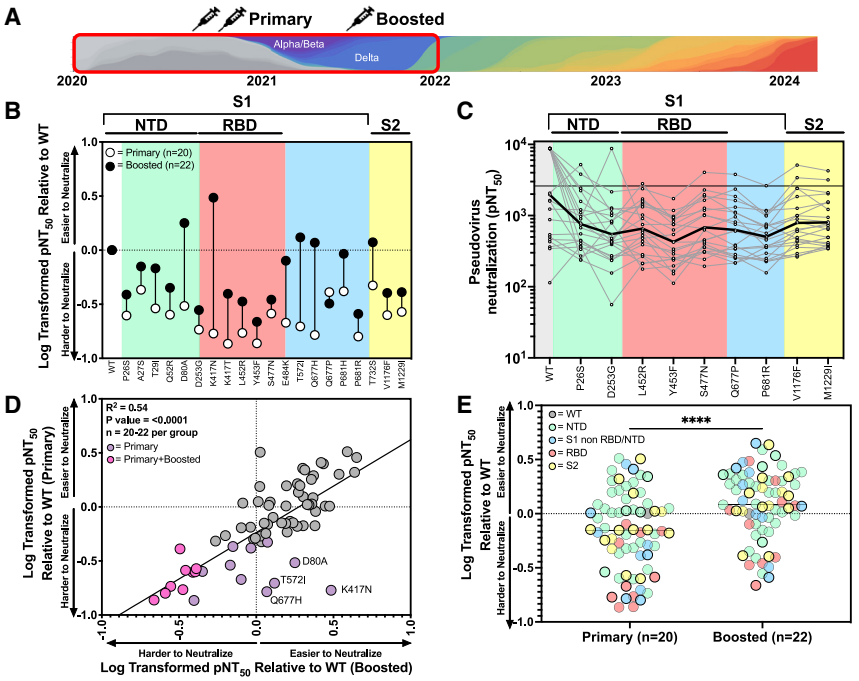

Figure 4. mRNA boosters significantly enhance neutralization of SARS-CoV-2 mutants

(A) (Top) schematic illustrating the time period from which variants were selected and the vaccinee sera to be tested below.

(B) (Bottom) primary or boosted pNT_{50} (n = 2) for donors across each variant was normalized to geometric mean titer across all donors for WT and log transformed. Length of each vertical line illustrates pNT_{50} change.

(C) Titers (n = 2 per sample per pseudovirus) that achieve 50% of pseudovirus neutralization (pNT_{50}) are plotted for mutants with significant escape boosted vaccination regimen found in SARS-CoV-2 through Delta (1.617.2). The solid black line represents geometric mean pNT_{50} for reference. The following abbreviations are used: NTD, N-terminal domain; RBD, receptor binding domain; S1, S1 subunit; S2, S2 subunit.

(D) Log-transformed pNT_{50} geometric mean values (average of n = 2) for each variant relative to WT for primary series were plotted against matching boosted values. Linear regression (R^2 = 0.5109; slope = −0.098; $p < 0.001$). Mutations that were escaped for primary vaccinees only or primary and boosted vaccinees are indicated. Labeled mutations are those that had the biggest change in pNT_{50} value relative to WT for boosted donors. Mutations that were escaped from primary series are highlighted in purple, and those that escape primary and boosted are pink.

(E) Log-transformed pNT_{50} geometric mean values (average of n = 2) for each variant relative to WT colored according to their location in the spike protein comparing primary to boosted vaccinee sera. Statistics represent Wilcoxon two-tailed paired, nonparametric t test with ****$p < 0.0001$. Selected RBD mutations from the delta and beta strains connected with lines showing their respective values for primary or boosted donor serum.

post-Delta were also significantly worse at binding to ACE2 vs. mutations pre-Delta (Figure S4B). Mapping these mutations onto the structure of the SARS-CoV-2 spike revealed that mutations appearing post-Delta were largely concentrated at the apex of the spike as well as parts of the NTD (Figure S4C). Neutralization titers of boosted sera against a panel of strains throughout the pandemic showed a 5-fold decrease in pNT_{50} value beginning with BA.1, further decreasing to 104-fold for the most escaped among them, BQ.1.1.22 (Figure S5A). In contrast to individual mutations, all strains exhibited improved ACE2 binding relative to the WT isolate, with Alpha and XBB descendants having the most significant increase (Figure S5B). When comparing neutralizing titer to ACE2 binding, all strains became harder to neutralize and better at binding to ACE2, with variants clustering on the plot by sequence similarity, but these trends were not significant (Figure 5E).

Bivalent and XBB.1.5 boosters markedly improve neutralization against recent variants in a nursing home cohort

During a surge in cases, largely attributed to the BA.5 variant, bivalent mRNA vaccines encoding both WT and BA.5 spike sequences were approved for use in the United States in August of 2022.[33,79] With the recombination of spikes producing XBB and sub-variants, and the waning immunity of bivalent vaccination against these variants,[80,81] a reformulated vaccine encoding only the XBB.1.5 spike sequence was recommended for use in September 2023.[82,83] We obtained longitudinal samples from 29 nursing home residents (median of 72 years old) and 7 health care workers (median age 60) who received either three or four WT mRNA vaccines followed by a bivalent booster and an XBB.1.5 booster (Table S4). To measure the impact of each vaccine administration, longitudinal serum samples, collected 2–4 weeks after vaccination, were tested against variants previously found to escape boosted sera, or which were dominant variants for more than a month (Figure 6A). While there was a clear trend of increased neutralizing activity with each successive vaccination, only modest differences were observed between the 3rd and 4th WT mRNA boost (Figure 6B). Bivalent vaccines improved pseudovirus neutralization titers after BA.5, though the activity against these variants was still significantly lower than WT (Figure S6A). While significantly improving titers against all variants up until JN.1, KP.2 and KP.3 showed significant escape from the XBB.1.5 boosted sera with KP.3 exhibiting 12.8-fold reduction in neutralizing titer. (Figure S6B). Overall, we observed increasing neutralization titers against all pseudoviruses tested relative to WT in the same cohort across each successive vaccination from WT booster to bivalent booster, and finally to XBB.1.5 booster (Figure 6C). We also observed a significant decline in neutralization activity across variants that arose across time for WT and bivalent boosters but no significant decline across variants following XBB.1.5 booster vaccination (Figure 6D). Two-way hierarchical clustering was performed on matched donors at the boosted time point to understand the effect of additional boosters against these variants (Figure 6E). Donors separated into two clusters after receiving a 3rd WT

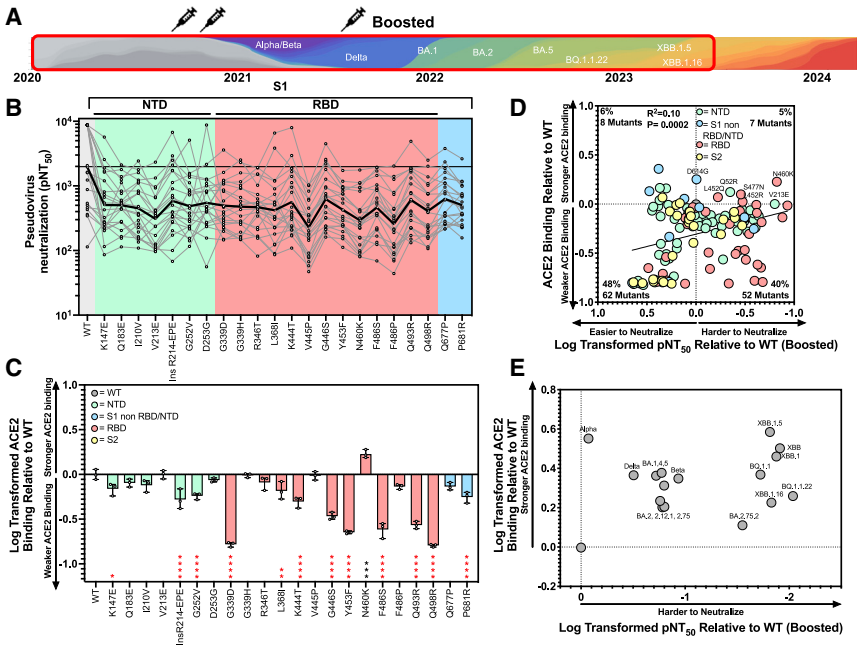

Figure 5. Individual Omicron variants reveal sites of resistance that are observed in more recent strains to significantly escape from boosted sera

(A) Schematic illustrating the time period from which variants were selected and the vaccinee sera to be tested below.

(B) pNT_{50} are plotted for all individual spike mutations occurring through XBB.1.16 variant with significant escape from 22 COVID naive boosted donors ($n = 2$ per sample per pseudovirus). The solid black line indicates the geometric mean of the titers against each pseudovirus. The following abbreviations are used: NTD, N-terminal domain; RBD, receptor binding domain; S1, S1 subunit; S2, S2 subunit.

(C) Individual pseudovirus mutants that escaped boosted vaccinees were measured for ACE2 binding. These values were then normalized to WT binding and log transformed. All experiments were performed in technical triplicates ($n = 3$). *, significantly worse ACE2 binding. Data are represented as mean ± SD (*$p < 0.0332$, **$p < 0.0021$, ***$p < 0.0002$, ****$p < 0.0001$).

(D) Neutralization titer relative to WT (average of $n = 2$) for boosted vaccinees was plotted against ACE2 binding relative to WT (average of $n = 3$). Both values are log transformed, and a correlation between them was detected with $p = 0.0002$. Numbers of mutations and percentages in each quadrant are listed, and mutations are colored according to their location on the spike.

(E) ACE binding relative to WT and infectivity relative to WT were plotted against each other. Each variant was tested in technical triplicates (average of $n = 3$). ACE2 binding and infectivity were assessed for correlation using a nonparametric two-tailed spearman correlation. $p = 0.33$.

booster, one with broader neutralizing activity and another with lower activity against BQ.1.1.22 and later strains. However, the distinction between these two clusters was largely attenuated with each successive administration of bivalent and XBB1.5 boosters. Taken together, these observations suggest that bivalent and XBB.1.5 boosters substantially improve the neutralization activity of sera against highly mutated variants.

SARS-CoV-2 variants of concern display increased ACE2 binding and infectivity over time

To compare variants of concern that were previously dominant or had escaped vaccines, we assessed ACE2 binding and the efficiency of viral entry mediated by the spike protein. All variants exhibited greater ACE2 binding than WT, but only strains arising after BQ.1.1.22 showed significant differences (Figure 7A). Notably, BA.2.86 and its descendant JN.1 had the strongest overall ACE2 binding, which was nearly 5-fold higher than WT. When analyzed relative to the date when each variant emerged, we found a significant correlation ($p = 0.0047$) between ACE2 binding and time, indicating that variants of concern increased their ACE2 binding over the course of the pandemic (Figure 7B).

To determine the ability of each spike to mediate viral entry into target cells expressing ACE2, we compared the rate of pseudovirus transduction over a range of concentrations (Figure S7A). We found that spikes ranging from BA.5 to HK.3 were significantly better at entering cells, mediating up to 30-fold more efficient cell entry than WT (Figure 7C). Notably, the highly mutated BA.2.86 spike was less efficient than preceding variants, but its descendant (JN.1) displayed 15-fold higher efficiency of cell entry than WT. Although we found no significant correlation between ACE2 binding and cell entry efficiency (Figure S7B), we observed that entry efficiency was significantly ($p = 0.0179$) correlated with time of variant emergence, indicating that variants of concern have become more efficient at cell entry over the course of the pandemic (Figure 7D).

DISCUSSION

Although the COVID-19 pandemic declaration was ended by the WHO in May 2023, SARS-CoV-2 continues to transmit globally in the form of highly mutated variants. We sought to understand how the constellation of mutations that have appeared since the beginning of the pandemic were impacted by the changing landscape of humoral immunity driven by updated vaccines. To this end, we determined the neutralization potency of patient sera against pseudoviruses representing 131 individual mutations from 50 named strains of SARS-CoV-2. Spike expression plasmids encoding each individual variant or strain have been deposited in a public repository that will make this resource freely available. Our study utilized this collection to characterize serum samples from COVID-naive donors who received a primary vaccination series, defined as either two shots of the Pfizer[28] or Moderna[29] mRNA vaccines or a third mRNA booster dose. We also analyzed longitudinal samples from a cohort consisting primarily of nursing home residents, taken after each successive vaccination. These individuals received up to a total of six mRNA vaccines, including the recent XBB.1.5 booster.

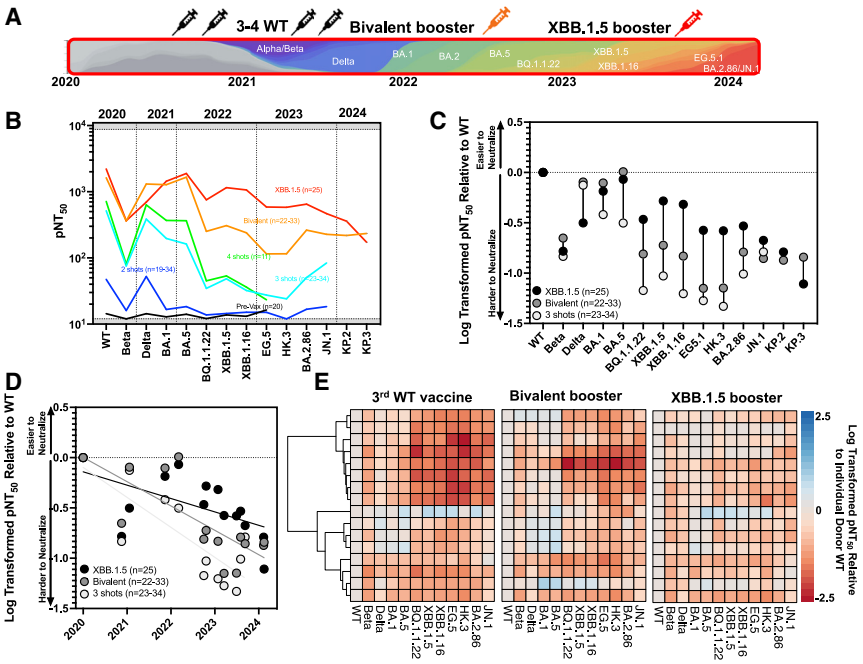

Figure 6. Updated COVID boosters improve neutralization against dominant variants throughout the pandemic

(A) Schematic illustrating the variants and vaccinee sera to be tested below.

(B) Geometric mean pNT_{50} values of longitudinal serum samples (average of $n = 2$) over the course of CDC-recommended vaccination schedule against each variant. Strains are plotted in the order in time that they first appear in GISAID.

(C) pNT_{50} of individual serum samples (average of $n = 2$) were normalized to geometric mean titer across all donors for WT and log transformed. Longitudinal samples from donors after WT, bivalent, or XBB.1.5 boosters are plotted. Length of each vertical line illustrates pNT_{50} change.

(D) Log-transformed pNT_{50} geometric mean values (average of $n = 2$) relative to WT for donor sera against variants of concern through JN.1 plotted against the date of first submission to GISAID. Solid lines represent linear regressions for WT booster ($R^2 = 0.63$, slope $= -0.298$, $p = 0.002$), bivalent booster ($R^2 = 0.57$, slope $= -0.24$, $p = 0.0018$), and XBB.1.5 booster titers ($R^2 = 0.31$, slope $= -0.133$, $p = 0.0379$).

(E) One-way hierarchical clustering of pNT_{50} values of sera obtained from boosted donors (rows) across each variant of concern (columns) relative to individual donor WT titer. Heatmaps maintaining clustering order of rows across bivalent and XBB.1.5 boosters are plotted to the right. pNT_{50} values are plotted in heatmaps colored according to neutralizing activity relative to WT. Clustering was performed using pheatmap package v1.0.12 in RStudio.

We find that sera from COVID-naive donors who received a primary vaccine series were especially vulnerable to individual mutations across multiple regions of the spike protein, including NTD, RBD, the C-terminal region of S1, and the C terminus of S2. Numerous individual mutations within the RBD resulted in significant escape from primary vaccination, many of which have been previously reported.[14,15,65] A majority of the single mutants through the Delta variant (82%) tested also exhibited lower ACE2 binding. This could be attributed to the expression at the surface of cells; however, most mutants expressed at a similar level to the WT virus. In agreement with others,[4,78,84,85] we found that D614G and H655Y conferred the greatest increase in ACE2 binding relative to the WT spike. D215G and ΔH69V70 mutants also increased ACE2 binding. Contrasting to the literature,[86] we observed that N501Y had significantly lower ACE2 binding relative to the WT. This difference could be attributed to a slightly lower expression of the N501Y mutant; however, most experiments have done binding with recombinantly expressed RBD while ours is done on the whole spike at the surface of the cell, which may explain this difference. Overall, our ACE2 binding data predominately agrees with what have been published. Notably, several mutants, including Q52R, L452R, S477N, T572I, D614G, H655Y, and H1101D, yielded both increased ACE2 binding and decreased neutralization. Specifically, three RBD mutations from the Beta variant (K417N, E484K, and N501Y) and two mutations from the Delta variant (L452R and P681R) substantially lowered the neutralization activity of sera from primary donors, in line with what others have observed.[12–15,17,20,21,46,65] The difference between the RBD double and triple mutants and the parent variants is likely due to the critical D614G mutation seen in all variants as well as P681R for Delta. Additionally, combinations of mutations had surprising effects on ACE2 binding, with the Beta triple-mutant RBD significantly increasing ACE2 binding in agreement with others[87] while the Delta double-mutant RBD significantly decreased ACE2 binding. Notably, the complete Delta strain had significantly higher ACE2 binding, suggesting that other mutations within Delta may have contributed to this difference and that the mutations are context dependent in their influence on ACE2 binding. Including the D614G and P681R mutant along with the RBD mutants would likely contribute to the increased ACE2 binding of the Delta variant.

A third mRNA booster dose exhibited significantly improved neutralization across many, but not all, of the individual mutants we tested. Fewer single mutations from Delta or earlier variants were able to significantly escape boosted serum, although there was still significant escape by D253G, L452R, S477N, Q677P, and P681R mutants, which have been previously characterized.[12,13,18–21,47,76,77] P26S, Y453F, V1176F, and M1229I mutants also significantly escaped boosted donor serum. Moreover, boosting disproportionately increased titers against specific key escape mutations across the spike including D80A, K417N, T572I, and Q677H. Recent publications have suggested that existing antibodies influence the outcome of vaccination by lowering the activation threshold for B cells to allow lower-affinity clones to participate as well as epitope masking to enable responses to previously ignored targets.[70] Although boosting resulted in substantially greater breadth of neutralization against more recent strains, we observed a distinct loss of activity for boosted sera beginning with the emergence of the BQ.1.1 variant. Interestingly, this appeared to be largely driven

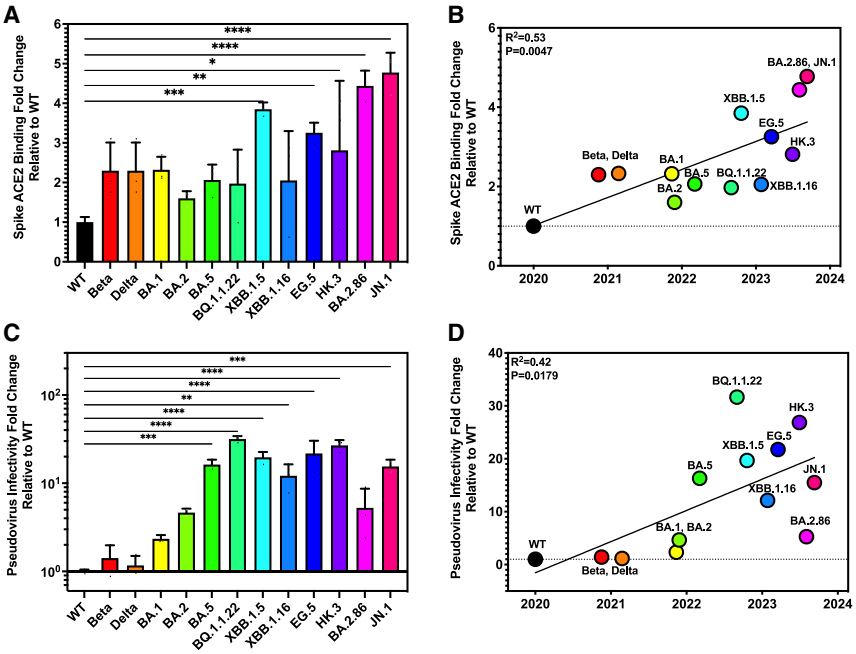

Figure 7. SARS-CoV-2 variants of concern have accumulated spike mutations increasing their infectivity and ACE2 binding over time

(A) Individual pseudovirus mutants were measured for ACE2 binding. All experiments were done in technical triplicates (n = 3). These values were then normalized to WT binding and compared to SARS-CoV-2 using a one-way ANOVA with Holm-Sidak correction for multiple comparisons. (* = p < 0.033, ** = p < 0.0021, *** = p < 0.0002, **** = p < 0.0001). Data are represented as mean ± SD.

(B) ACE2 binding values (average of n = 3) plotted for each variant relative to the time it was first submitted to the GISAID database. A simple linear regression was performed with R^2 = 0.53, p = 0.0047, slope = 0.707.

(C) Pseudovirus infectivity (defined as infectious units per genome copy) was normalized to WT infectivity for each variant spike across technical triplicates (n = 3). Pseudovirus infectivity relative to WT was measured for major SARS-CoV-2 variants by calculating fold change in slope of linear regressions fit across known dilutions. Bars and error bars depict mean and standard error of the mean. Each pseudovirus was compared to SARS-CoV-2 wild type using a one-way ANOVA with Holm-Sidak correction for multiple comparisons. (* = p < 0.033, ** = p < 0.0021, *** = p < 0.0002, **** = p < 0.0001). Data are represented as mean ± SD.

(D) Pseudovirus infectivity values (average of n = 3) plotted for each variant relative to the time it was first submitted to the GISAID database. A simple linear regression was performed with R^2 = 0.42, p = 0.0179, and slope = 5.89.

by RBD and NTD mutations at positions 213, 445, 460, and 486, which have been retained in all variants since XBB. Interestingly, these four mutations achieved neutralization resistance without the loss of ACE2 binding in our assay. Moreover, mutations that appear after the Delta variant mostly reduced ACE2 binding aside from the previously reported N460K.[40] In agreement with others,[87–90] when we measured variant binding to ACE2, all variants had increased binding relative to the WT. Significantly, this finding indicates that mutations coordinate together in the context of each variant backbone, which could explain why most single mutants decreased ACE2 binding in our assays. More work needs to be done to understand mutant binding to ACE2 in the context of each variant rather than in the WT plasmid backbone.

In response to the rapid emergence of SARS-CoV-2 variants, the vaccine formulation was twice updated, first to deliver a bivalent immunogen containing spike proteins from the WT and BA.4/BA.5 strains[91,92] and then again to deliver a monovalent XBB.1.5 spike sequence.[82,83] We found that bivalent booster results in neutralizing activity comparable to WT for variants BA.5 and earlier, while also improving activity against BQ.1.1 and later variants. However, these later variants still significantly escaped bivalent booster vaccination and had increased ACE2 binding. In contrast, we found that the XBB.1.5 booster results in substantial neutralization potency against later variants and only saw significant escape against Beta and the more recent JN.1 variant.

In addition to mediating escape from vaccine sera, we found that spike mutations also contribute significantly to the ability of pseudovirus to infect cells and bind ACE2, suggesting that viral evolution is optimizing antibody escape, receptor binding, and viral entry simultaneously. We found that spikes from variants post-BA.1 produced pseudoviruses that were up to 30-fold better at transducing target cells than WT, suggesting that WT SARS-CoV-2 spike was not optimally configured for ACE2-dependent viral entry. Additionally, we found that variants exhibited up to 5-fold better ACE2 binding by spikes expressed on the surface of cells, although ACE2 binding and infectivity were not significantly correlated despite there being a general trend toward better receptor binding and pseudovirus entry.

Our comprehensive study demonstrates that individuals receiving the full mRNA vaccination regimen, including the XBB.1.5 booster, have maximally effective neutralizing activity against recent strains of SARS-CoV-2. However, despite improvements mediated by XBB.1.5 boosters against more recently emerging strains, there is still escape, particularly by the latest JN.1 descendants KP.2 and KP.3. Surprisingly, the beta variant was also able to significantly escape both bivalent- and XBB.1.5-boosted donors. Notably, the mutations from the beta variant not seen in later variants that significantly escaped include L18F, D80A, D215G, del242-244, and A701V. These results indicate that there still exists a risk of a previous variant reemerging, although likely with a lower fitness than the current variants. These results highlight the ongoing challenge presented by continued evolution of SARS-CoV-2, which has outpaced attempts to update vaccines. Our findings support the development of vaccine and prevention modalities capable of eliciting broad protection against future variants/outbreaks. Of note, a number of monoclonal antibodies have been described that target highly

conserved epitopes such as the stem helix[93–96] or fusion peptide,[97–100] which are capable of neutralizing across the entire *Coronaviridae* family. Next-generation vaccines that exploit these and other sites of vulnerability across coronaviruses will likely be necessary to combat the ongoing evolution of SARS-CoV-2 and may help prevent future pandemics.

Limitations of the study

While numerous prior studies have shown that neutralization activity against pseudoviruses is well correlated to replication competent SARS-CoV-2,[60–64] it is possible that the mutations in the more recent variant spike proteins may cause them to behave differently than previously tested variants. In addition, while we confirmed that ACE2 expression is required for infection of 293T cells, natural target cells in the respiratory tract may express alternative receptors or attachment factors that facilitate infection and are not adequately modeled in our system. The study is limited to the evaluation of serum neutralizing antibodies to the spike protein for our pseudovirus neutralization assay and does not take into account neutralizing antibodies to other proteins including the N and M proteins. We also only assessed mutations in the context of the WT spike as a backbone, and there may be substantial differences in ACE2 binding of individual mutations in the context of other variant backbones such as BA.5 or XBB.1.5. Furthermore, it is possible that expression of spike at the cell surface can have an impact on ACE2 binding although most of our single mutants expressed at levels similar to the WT spike. Moreover, when assessing combinations of mutations, we only included combinations of RBD mutations within the Beta and Delta variants and did not directly test these with the addition of the D614G mutant. Given that this was the first mutation made by the virus, our study of these combinations is limited by the omission of these and could be considered to not accurately represent the variants. However, our goal was to assess the effects of the combinations of RBD mutations in the context of the WT backbone, and as such, we saw that the combinations of RBD mutants almost completely recapitulated what was seen in the full variant. Additionally, our infectivity studies only take into account the infectivity of spike mutations, not mutations in other proteins that contribute to viral infectivity. Furthermore, we did not assess other antibody-mediated functions such as complement deposition, antibody-dependent cellular cytotoxicity, or antibody-dependent cellular phagocytosis, which may contribute to protection even in the absence of neutralizing antibodies. Nor did we assess the role of vaccine-elicited cellular immune responses mediated by T cells and natural killer cells, which are likely to play a key role in disease prevention for vaccine recipients. Another limitation of the study is that the primary and boosted cohorts were COVID naive and therefore could not account for the impact of hybrid immunity. Our goal was to deeply profile the effect of vaccination on humoral immunity to COVID, so we purposefully excluded any donors that previously tested positive for COVID. For the nursing home cohort, these donors do have a COVID history, and we cannot rule out that this history has contributed to their neutralizing activity over time as they were infected between or before vaccination. We included this cohort to take a bird's eye view of all strains throughout the entire pandemic.

RESOURCE AVAILABILITY

Lead contact

Further information and requests for resources and reagents should be directed to and will be fulfilled by Alejandro Balazs (abalazs@mgh.harvard.edu).

Materials availability

Plasmids generated in this study are available through Addgene. Recombinant proteins and antibodies are available from their respective sources.

Data and code availability

This study did not generate sequence data. Data generated in the current study (including neutralization measurements and flow cytometric files) have not been deposited in a public repository but are available from the corresponding author upon request. The code used to generate the clustered heatmaps can be made available from the corresponding author upon request. Any additional information required to reanalyze the data reported in this work paper is available from the lead contact upon request.

ACKNOWLEDGMENTS

We wish to thank Michael Farzan, PhD, for providing ACE2-expressing 293T cells. This work was supported by the Peter and Ann Lambertus Family Foundation. A.B.B. was supported by NIAID R01s AI174875 and AI174276, the NIDA Avenir New Innovator Award DP2DA040254, the NIDA Avant-Garde Award 1DP1DA060607, a Massachusetts Consortium on Pathogen Readiness grant, CDC subcontract 200-2016-91773-T.O.2, and a grant from Coalition for Epidemic Preparedness Innovations.

AUTHOR CONTRIBUTIONS

Conceptualization: A.L.R., Y.C., W.F.G.-B., and A.B.B. Methodology: A.L.R., Y.C., K.S.D., M.L.S., and E.C.L. Samples: D.J.G., M.C.P., A.J.I., D.H.C., S.G., and W.F.G.-B. Investigation: A.L.R., Y.C., C.J.L., K.S.D., M.L.S., and E.C.L. Data curation: A.L.R., Y.C., K.S.D., and M.L.S. Writing – original draft: A.L.R. Writing – reviewing and editing: A.L.R., Y.C., and A.B.B. edited the paper with input from co-authors.

DECLARATION OF INTERESTS

A.B.B. is a founder of Cure Systems LLC.

STAR★METHODS

Detailed methods are provided in the online version of this paper and include the following:

- KEY RESOURCES TABLE
- EXPERIMENTAL MODEL AND STUDY PARTICIPANT DETAILS
  - Human subjects
  - Cell lines
- METHOD DETAILS
  - Construction of variant spike expression plasmids
  - SARS-CoV-2 pseudovirus neutralization assay
  - Titering
  - Quantitation of pseudovirus by RT-qPCR
  - ACE2 spike binding
- QUANTIFICATION AND STATISTICAL ANALYSIS

SUPPLEMENTAL INFORMATION

Supplemental information can be found online at https://doi.org/10.1016/j.xcrm.2024.101850.

Received: September 13, 2024
Revised: October 24, 2024
Accepted: November 12, 2024
Published: December 9, 2024

REFERENCES

1. Cucinotta, D., and Vanelli, M. (2020). WHO Declares COVID-19 a Pandemic. Acta Biomed. *91*, 157–160. https://doi.org/10.23750/abm.v91i1.9397.
2. WHO Coronavirus (COVID-19) Dashboard https://covid19.who.int.
3. Worldometers, info (2023). Worldometer - FAQ. https://www.worldometers.info/faq/.
4. Korber, B., Fischer, W.M., Gnanakaran, S., Yoon, H., Theiler, J., Abfalterer, W., Hengartner, N., Giorgi, E.E., Bhattacharya, T., Foley, B., et al. (2020). Tracking Changes in SARS-CoV-2 Spike: Evidence that D614G Increases Infectivity of the COVID-19 Virus. Cell *182*, 812–827.e19. https://doi.org/10.1016/j.cell.2020.06.043.
5. Plante, J.A., Liu, Y., Liu, J., Xia, H., Johnson, B.A., Lokugamage, K.G., Zhang, X., Muruato, A.E., Zou, J., Fontes-Garfias, C.R., et al. (2021). Spike mutation D614G alters SARS-CoV-2 fitness. Nature *592*, 116–121. https://doi.org/10.1038/s41586-020-2895-3.
6. Qassim, S.H., Hasan, M.R., Tang, P., Chemaitelly, H., Ayoub, H.H., Yassine, H.M., Al-Khatib, H.A., Smatti, M.K., Abdul-Rahim, H.F., Nasrallah, G.K., et al. (2022). Effects of SARS-CoV-2 Alpha, Beta, and Delta variants, age, vaccination, and prior infection on infectiousness of SARS-CoV-2 infections. Front. Immunol. *13*, 984784.
7. Rajah, M.M., Hubert, M., Bishop, E., Saunders, N., Robinot, R., Grzelak, L., Planas, D., Dufloo, J., Gellenoncourt, S., Bongers, A., et al. (2021). SARS-CoV-2 Alpha, Beta, and Delta variants display enhanced Spike-mediated syncytia formation. EMBO J. *40*, e108944. https://doi.org/10.15252/embj.2021108944.
8. Trobajo-Sanmartín, C., Martínez-Baz, I., Miqueleiz, A., Fernández-Huerta, M., Burgui, C., Casado, I., Baigorría, F., Navascués, A., Castilla, J., and Ezpeleta, C. (2022). Differences in Transmission between SARS-CoV-2 Alpha (B.1.1.7) and Delta (B.1.617.2) Variants. Microbiol. Spectr. *10*, e00008-22. https://doi.org/10.1128/spectrum.00008-22.
9. Mlcochova, P., Kemp, S.A., Dhar, M.S., Papa, G., Meng, B., Ferreira, I.A.T.M., Datir, R., Collier, D.A., Albecka, A., Singh, S., et al. (2021). SARS-CoV-2 B.1.617.2 Delta variant replication and immune evasion. Nature *599*, 114–119. https://doi.org/10.1038/s41586-021-03944-y.
10. Garcia-Beltran, W.F., Lam, E.C., St. Denis, K., Nitido, A.D., Garcia, Z.H., Hauser, B.M., Feldman, J., Pavlovic, M.N., Gregory, D.J., Poznansky, M.C., et al. (2021). Multiple SARS-CoV-2 variants escape neutralization by vaccine-induced humoral immunity. Cell *184*, 2372–2383.e9. https://doi.org/10.1016/j.cell.2021.03.013.
11. Newman, J., Thakur, N., Peacock, T.P., Bialy, D., Elrefaey, A.M.E., Bogaardt, C., Horton, D.L., Ho, S., Kankeyan, T., Carr, C., et al. (2022). Neutralizing antibody activity against 21 SARS-CoV-2 variants in older adults vaccinated with BNT162b2. Nat. Microbiol. *7*, 1180–1188. https://doi.org/10.1038/s41564-022-01163-3.
12. Zhang, Y., Zhang, T., Fang, Y., Liu, J., Ye, Q., and Ding, L. (2022). SARS-CoV-2 spike L452R mutation increases Omicron variant fusogenicity and infectivity as well as host glycolysis. Signal Transduct. Target. Ther. *7*, 76. https://doi.org/10.1038/s41392-022-00941-z.
13. Tchesnokova, V., Kulasekara, H., Larson, L., Bowers, V., Rechkina, E., Kisiela, D., Sledneva, Y., Choudhury, D., Maslova, I., Deng, K., et al. (2021). Acquisition of the L452R Mutation in the ACE2-Binding Interface of Spike Protein Triggers Recent Massive Expansion of SARS-CoV-2 Variants. J. Clin. Microbiol. *59*, e0092121. https://doi.org/10.1128/JCM.00921-21.
14. Harvey, W.T., Carabelli, A.M., Jackson, B., Gupta, R.K., Thomson, E.C., Harrison, E.M., Ludden, C., Reeve, R., Rambaut, A., et al.; COVID-19 Genomics UK COG-UK Consortium (2021). SARS-CoV-2 variants, spike mutations and immune escape. Nat. Rev. Microbiol. *19*, 409–424. https://doi.org/10.1038/s41579-021-00573-0.
15. Xue, S., Han, Y., Wu, F., and Wang, Q. (2024). Mutations in the SARS-CoV-2 spike receptor binding domain and their delicate balance between ACE2 affinity and antibody evasion. Protein Cell *15*, 403–418, pwae007. https://doi.org/10.1093/procel/pwae007.
16. Greaney, A.J., Loes, A.N., Crawford, K.H.D., Starr, T.N., Malone, K.D., Chu, H.Y., and Bloom, J.D. (2021). Comprehensive mapping of mutations in the SARS-CoV-2 receptor-binding domain that affect recognition by polyclonal human plasma antibodies. Cell Host Microbe *29*, 463–476.e6. https://doi.org/10.1016/j.chom.2021.02.003.
17. Starr, T.N., Greaney, A.J., Hilton, S.K., Ellis, D., Crawford, K.H.D., Dingens, A.S., Navarro, M.J., Bowen, J.E., Tortorici, M.A., Walls, A.C., et al. (2020). Deep Mutational Scanning of SARS-CoV-2 Receptor Binding Domain Reveals Constraints on Folding and ACE2 Binding. Cell *182*, 1295–1310.e20. https://doi.org/10.1016/j.cell.2020.08.012.
18. Zeng, C., Evans, J.P., Faraone, J.N., Qu, P., Zheng, Y.-M., Saif, L., Oltz, E.M., Lozanski, G., Gumina, R.J., and Liu, S.-L. (2021). Neutralization of SARS-CoV-2 Variants of Concern Harboring Q677H. mBio *12*, e0251021. https://doi.org/10.1128/mbio.02510-21.
19. Niu, X., Xu, J., Liu, M., Tu, H., Koenig, S.N., Saif, L.J., Jones, D.M., and Wang, Q. (2022). Isolation and characterization of a SARS-CoV-2 variant with a Q677H mutation in the spike protein. Arch. Virol. *168*, 5. https://doi.org/10.1007/s00705-022-05621-5.
20. Furusawa, Y., Kiso, M., Iida, S., Uraki, R., Hirata, Y., Imai, M., Suzuki, T., Yamayoshi, S., and Kawaoka, Y. (2023). SARS-CoV-2 delta variants, Spike-P681R and D950N promote membrane fusion, Spike-P681R enhances spike cleavage, but neither substitution affects pathogenicity in hamsters. EBioMedicine *91*, 104561. https://doi.org/10.1016/j.ebiom.2023.104561.
21. Saito, A., Irie, T., Suzuki, R., Maemura, T., Nasser, H., Uriu, K., Kosugi, Y., Shirakawa, K., Sadamasu, K., Kimura, I., et al. (2022). Enhanced fusogenicity and pathogenicity of SARS-CoV-2 Delta P681R mutation. Nature *602*, 300–306. https://doi.org/10.1038/s41586-021-04266-9.
22. Cele, S., Gazy, I., Jackson, L., Hwa, S.-H., Tegally, H., Lustig, G., Giandhari, J., Pillay, S., Wilkinson, E., Naidoo, Y., et al. (2021). Escape of SARS-CoV-2 501Y.V2 from neutralization by convalescent plasma. Nature *593*, 142–146. https://doi.org/10.1038/s41586-021-03471-w.
23. Garcia-Beltran, W.F., St. Denis, K.J., Hoelzemer, A., Lam, E.C., Nitido, A.D., Sheehan, M.L., Berrios, C., Ofoman, O., Chang, C.C., Hauser, B.M., et al. (2022). mRNA-based COVID-19 vaccine boosters induce neutralizing immunity against SARS-CoV-2 Omicron variant. Cell *185*, 457–466.e4. https://doi.org/10.1016/j.cell.2021.12.033.
24. Zhou, D., Dejnirattisai, W., Supasa, P., Liu, C., Mentzer, A.J., Ginn, H.M., Zhao, Y., Duyvesteyn, H.M.E., Tuekprakhon, A., Nutalai, R., et al. (2021). Evidence of escape of SARS-CoV-2 variant B.1.351 from natural and vaccine-induced sera. Cell *184*, 2348–2361.e6. https://doi.org/10.1016/j.cell.2021.02.037.
25. Faraone, J.N., Qu, P., Evans, J.P., Zheng, Y.-M., Carlin, C., Anghelina, M., Stevens, P., Fernandez, S., Jones, D., Lozanski, G., et al. (2023). Neutralization escape of Omicron XBB, BR.2, and BA.2.3.20 subvariants. Cell Rep. Med. *4*, 101049. https://doi.org/10.1016/j.xcrm.2023.101049.
26. Pallesen, J., Wang, N., Corbett, K.S., Wrapp, D., Kirchdoerfer, R.N., Turner, H.L., Cottrell, C.A., Becker, M.M., Wang, L., Shi, W., et al. (2017). Immunogenicity and structures of a rationally designed prefusion MERS-CoV spike antigen. Proc. Natl. Acad. Sci. *114*, E7348–E7357. https://doi.org/10.1073/pnas.1707304114.
27. Hsieh, C.-L., Goldsmith, J.A., Schaub, J.M., DiVenere, A.M., Kuo, H.-C., Javanmardi, K., Le, K.C., Wrapp, D., Lee, A.G., Liu, Y., et al. (2020).

Structure-based design of prefusion-stabilized SARS-CoV-2 spikes. Science *369*, 1501–1505. https://doi.org/10.1126/science.abd0826.

28. Polack, F.P., Thomas, S.J., Kitchin, N., Absalon, J., Gurtman, A., Lockhart, S., Perez, J.L., Pérez Marc, G., Moreira, E.D., Zerbini, C., et al. (2020). Safety and Efficacy of the BNT162b2 mRNA Covid-19 Vaccine. N. Engl. J. Med. *383*, 2603–2615.
29. Baden, L.R., El Sahly, H.M., Essink, B., Kotloff, K., Frey, S., Novak, R., Diemert, D., Spector, S.A., Rouphael, N., Creech, C.B., et al. (2021). Efficacy and Safety of the mRNA-1273 SARS-CoV-2 Vaccine. N. Engl. J. Med. *384*, 403–416. https://doi.org/10.1056/NEJMoa2035389.
30. Heath, P.T., Galiza, E.P., Baxter, D.N., Boffito, M., Browne, D., Burns, F., Chadwick, D.R., Clark, R., Cosgrove, C., Galloway, J., et al. (2021). Safety and Efficacy of NVX-CoV2373 Covid-19 Vaccine. N. Engl. J. Med. *385*, 1172–1183.
31. Sadoff, J., Gray, G., Vandebosch, A., Cárdenas, V., Shukarev, G., Grinsztejn, B., Goepfert, P.A., Truyers, C., Fennema, H., Spiessens, B., et al. (2021). Safety and Efficacy of Single-Dose Ad26.COV2.S Vaccine against Covid-19. N. Engl. J. Med. *384*, 2187–2201.
32. Bar-On, Y.M., Goldberg, Y., Mandel, M., Bodenheimer, O., Freedman, L., Kalkstein, N., Mizrahi, B., Alroy-Preis, S., Ash, N., Milo, R., and Huppert, A. (2021). Protection of BNT162b2 Vaccine Booster against Covid-19 in Israel. N. Engl. J. Med. *385*, 1393–1400.
33. Tartof, S.Y., Slezak, J.M., Puzniak, L., Hong, V., Frankland, T.B., Ackerson, B.K., Takhar, H., Ogun, O.A., Simmons, S., Zamparo, J.M., et al. (2022). BNT162b2 vaccine effectiveness against SARS-CoV-2 omicron BA.4 and BA.5. Lancet Infect. Dis. *22*, 1663–1665. https://doi.org/10.1016/S1473-3099(22)00692-2.
34. COVID-19 Vaccination (2023). Cent. Dis. Control Prev. https://www.cdc.gov/coronavirus/2019-ncov/vaccines/stay-up-to-date.html.
35. Miller, J., Hachmann, N.P., Collier, A.R.Y., Lasrado, N., Mazurek, C.R., Patio, R.C., Powers, O., Surve, N., Theiler, J., Korber, B., and Barouch, D.H. (2023). Substantial Neutralization Escape by SARS-CoV-2 Omicron Variants BQ.1.1 and XBB.1. N. Engl. J. Med. *388*, 662–664.
36. Jeworowski, L.M., Mühlemann, B., Walper, F., Schmidt, M.L., Jansen, J., Krumbholz, A., Simon-Lorière, E., Jones, T.C., Corman, V.M., and Drosten, C. (2024). Humoral immune escape by current SARS-CoV-2 variants BA.2.86 and JN.1, December 2023. Euro Surveill. *29*, 2300740. https://doi.org/10.2807/1560-7917.ES.2024.29.2.2300740.
37. Lasrado, N., Collier, A.-R.Y., Hachmann, N.P., Miller, J., Rowe, M., Schonberg, E.D., Rodrigues, S.L., LaPiana, A., Patio, R.C., Anand, T., et al. (2023). Neutralization escape by SARS-CoV-2 Omicron subvariant BA.2.86. Vaccine *41*, 6904–6909. https://doi.org/10.1016/j.vaccine.2023.10.051.
38. Chen, S., Huang, Z., Guo, Y., Guo, H., Jian, L., Xiao, J., Yao, X., Yu, H., Cheng, T., Zhang, Y., et al. (2023). Evolving spike mutations in SARS-CoV-2 Omicron variants facilitate evasion from breakthrough infection-acquired antibodies. Cell Discov. *9*, 86. https://doi.org/10.1038/s41421-023-00584-6.
39. Alcantara, M.C., Higuchi, Y., Kirita, Y., Matoba, S., and Hoshino, A. (2023). Deep Mutational Scanning to Predict Escape from Bebtelovimab in SARS-CoV-2 Omicron Subvariants. Vaccines *11*, 711. https://doi.org/10.3390/vaccines11030711.
40. Qu, P., Evans, J.P., Zheng, Y.-M., Carlin, C., Saif, L.J., Oltz, E.M., Xu, K., Gumina, R.J., and Liu, S.-L. (2022). Evasion of neutralizing antibody responses by the SARS-CoV-2 BA.2.75 variant. Cell Host Microbe *30*, 1518–1526.e4. https://doi.org/10.1016/j.chom.2022.09.015.
41. Parums, D.V. (2023). Editorial: The XBB.1.5 ('Kraken') Subvariant of Omicron SARS-CoV-2 and its Rapid Global Spread. Med. Med. Sci. Monit. *29*, e939580. https://doi.org/10.12659/MSM.939580.
42. Focosi, D., Quiroga, R., McConnell, S., Johnson, M.C., and Casadevall, A. (2023). Convergent Evolution in SARS-CoV-2 Spike Creates a Variant Soup from Which New COVID-19 Waves Emerge. Int. J. Mol. Sci. *24*, 2264. https://doi.org/10.3390/ijms24032264.
43. Qu, P., Evans, J.P., Faraone, J.N., Zheng, Y.-M., Carlin, C., Anghelina, M., Stevens, P., Fernandez, S., Jones, D., Lozanski, G., et al. (2023). Enhanced neutralization resistance of SARS-CoV-2 Omicron subvariants BQ.1, BQ.1.1, BA.4.6, BF.7, and BA.2.75.2. Cell Host Microbe *31*, 9–17.e3. https://doi.org/10.1016/j.chom.2022.11.012.
44. Wang, Q., Guo, Y., Iketani, S., Nair, M.S., Li, Z., Mohri, H., Wang, M., Yu, J., Bowen, A.D., Chang, J.Y., et al. (2022). Antibody evasion by SARS-CoV-2 Omicron subvariants BA.2.12.1, BA.4 and BA.5. Nature *608*, 603–608. https://doi.org/10.1038/s41586-022-05053-w.
45. Cao, Y., Wang, J., Jian, F., Xiao, T., Song, W., Yisimayi, A., Huang, W., Li, Q., Wang, P., An, R., et al. (2022). Omicron escapes the majority of existing SARS-CoV-2 neutralizing antibodies. Nature *602*, 657–663. https://doi.org/10.1038/s41586-021-04385-3.
46. Alam, M.M., Hannan, S.B., Saikat, T.A., Limon, M.B.H., Topu, M.R., Rana, M.J., Salauddin, A., Bosu, S., and Rahman, M.Z. (2023). Beta, Delta, and Omicron, Deadliest Among SARS-CoV-2 Variants: A Computational Repurposing Approach. Evol. Bioinform. Online *19*, 11769343231182258. https://doi.org/10.1177/11769343231182258.
47. Wang, Q., Ye, S.-B., Zhou, Z.-J., Song, A.-L., Zhu, X., Peng, J.-M., Liang, R.-M., Yang, C.-H., Yu, X.-W., Huang, X., et al. (2023). Key mutations in the spike protein of SARS-CoV-2 affecting neutralization resistance and viral internalization. J. Med. Virol. *95*, e28407. https://doi.org/10.1002/jmv.28407.
48. Wang, Q., Iketani, S., Li, Z., Guo, Y., Yeh, A.Y., Liu, M., Yu, J., Sheng, Z., Huang, Y., Liu, L., and Ho, D.D. (2022). Antigenic characterization of the SARS-CoV-2 Omicron subvariant BA.2.75. Cell Host Microbe *30*, 1512–1517.e4. https://doi.org/10.1016/j.chom.2022.09.002.
49. Ao, D., He, X., Hong, W., and Wei, X. (2023). The rapid rise of SARS-CoV-2 Omicron subvariants with immune evasion properties: XBB.1.5 and BQ.1.1 subvariants. MedComm. *4*, e239. https://doi.org/10.1002/mco2.239.
50. Thomson, E.C., Rosen, L.E., Shepherd, J.G., Spreafico, R., da Silva Filipe, A., Wojcechowskyj, J.A., Davis, C., Piccoli, L., Pascall, D.J., Dillen, J., et al. (2021). Circulating SARS-CoV-2 spike N439K variants maintain fitness while evading antibody-mediated immunity. Cell *184*, 1171–1187.e20. https://doi.org/10.1016/j.cell.2021.01.037.
51. Verma, S., Patil, V.M., and Gupta, M.K. (2022). Mutation informatics: SARS-CoV-2 receptor-binding domain of the spike protein. Drug Discov. Today *27*, 103312. https://doi.org/10.1016/j.drudis.2022.06.012.
52. Bate, N., Savva, C.G., Moody, P.C.E., Brown, E.A., Evans, S.E., Ball, J.K., Schwabe, J.W.R., Sale, J.E., and Brindle, N.P.J. (2022). In vitro evolution predicts emerging SARS-CoV-2 mutations with high affinity for ACE2 and cross-species binding. PLoS Pathog. *18*, e1010733. https://doi.org/10.1371/journal.ppat.1010733.
53. Center for Biologics Evaluation and Research (CBER) (2023). Updated COVID-19 Vaccines for Use in the United States Beginning in Fall 2023 (FDA).
54. GISAID Initiative https://www.epicov.org/epi3/frontend#b40c.
55. Hadfield, J., Megill, C., Bell, S.M., Huddleston, J., Potter, B., Callender, C., Sagulenko, P., Bedford, T., and Neher, R.A. (2018). Nextstrain: real-time tracking of pathogen evolution. Bioinformatics *34*, 4121–4123. https://doi.org/10.1093/bioinformatics/bty407.
56. Garcia-Beltran, W.F., Lam, E.C., Astudillo, M.G., Yang, D., Miller, T.E., Feldman, J., Hauser, B.M., Caradonna, T.M., Clayton, K.L., Nitido, A.D., et al. (2021). COVID-19-neutralizing antibodies predict disease severity and survival. Cell *184*, 476–488.e11. https://doi.org/10.1016/j.cell.2020.12.015.
57. Cantoni, D., Mayora-Neto, M., Thakur, N., Elrefaey, A.M.E., Newman, J., Vishwanath, S., Nadesalingam, A., Chan, A., Smith, P., Castillo-Olivares, J., et al. (2022). Pseudotyped Bat Coronavirus RaTG13 is efficiently neutralised by convalescent sera from SARS-CoV-2 infected patients. Commun. Biol. *5*, 409. https://doi.org/10.1038/s42003-022-03325-9.

58. Wrobel, A.G., Benton, D.J., Xu, P., Roustan, C., Martin, S.R., Rosenthal, P.B., Skehel, J.J., and Gamblin, S.J. (2020). SARS-CoV-2 and bat RaTG13 spike glycoprotein structures inform on virus evolution and furin-cleavage effects. Nat. Struct. Mol. Biol. *27*, 763–767. https://doi.org/10.1038/s41594-020-0468-7.

59. Cai, Y., Zhang, J., Xiao, T., Peng, H., Sterling, S.M., Walsh, R.M., Rawson, S., Rits-Volloch, S., and Chen, B. (2020). Distinct conformational states of SARS-CoV-2 spike protein. Science *369*, 1586–1592. https://doi.org/10.1126/science.abd4251.

60. Crawford, K.H.D., Eguia, R., Dingens, A.S., Loes, A.N., Malone, K.D., Wolf, C.R., Chu, H.Y., Tortorici, M.A., Veesler, D., Murphy, M., et al. (2020). Protocol and Reagents for Pseudotyping Lentiviral Particles with SARS-CoV-2 Spike Protein for Neutralization Assays. Viruses *12*, 513. https://doi.org/10.3390/v12050513.

61. Ju, B., Zhang, Q., Ge, J., Wang, R., Sun, J., Ge, X., Yu, J., Shan, S., Zhou, B., Song, S., et al. (2020). Human neutralizing antibodies elicited by SARS-CoV-2 infection. Nature *584*, 115–119. https://doi.org/10.1038/s41586-020-2380-z.

62. Pinto, D., Park, Y.-J., Beltramello, M., Walls, A.C., Tortorici, M.A., Bianchi, S., Jaconi, S., Culap, K., Zatta, F., De Marco, A., et al. (2020). Cross-neutralization of SARS-CoV-2 by a human monoclonal SARS-CoV antibody. Nature *583*, 290–295. https://doi.org/10.1038/s41586-020-2349-y.

63. Wang, C., Li, W., Drabek, D., Okba, N.M.A., van Haperen, R., Osterhaus, A.D.M.E., van Kuppeveld, F.J.M., Haagmans, B.L., Grosveld, F., and Bosch, B.-J. (2020). A human monoclonal antibody blocking SARS-CoV-2 infection. Nat. Commun. *11*, 2251. https://doi.org/10.1038/s41467-020-16256-y.

64. Yang, R., Huang, B., Ruhan, A., Li, W., Wang, W., Deng, Y., and Tan, W. (2020). Development and effectiveness of pseudotyped SARS-CoV-2 system as determined by neutralizing efficiency and entry inhibition test in vitro. Biosaf. Health *2*, 226–231. https://doi.org/10.1016/j.bsheal.2020.08.004.

65. Mohammadi, M., Shayestehpour, M., and Mirzaei, H. (2021). The impact of spike mutated variants of SARS-CoV2 [Alpha, Beta, Gamma, Delta, and Lambda] on the efficacy of subunit recombinant vaccines. Braz. J. Infect. Dis. *25*, 101606. https://doi.org/10.1016/j.bjid.2021.101606.

66. Majumdar, P., and Niyogi, S. (2021). SARS-CoV-2 mutations: the biological trackway towards viral fitness. Epidemiol. Infect. *149*, e110. https://doi.org/10.1017/S0950268821001060.

67. Commissioner (2021). FDA Authorizes Booster Dose of Pfizer-BioNTech COVID-19 Vaccine for Certain Populations (FDA). https://www.fda.gov/news-events/press-announcements/fda-authorizes-booster-dose-pfizer-biontech-covid-19-vaccine-certain-populations.

68. Wesemann, D.R. (2022). Omicron's message on vaccines: Boosting begets breadth. Cell *185*, 411–413. https://doi.org/10.1016/j.cell.2022.01.006.

69. Nair, M.S., Ribeiro, R.M., Wang, M., Bowen, A.D., Liu, L., Guo, Y., Chang, J.Y., Wang, P., Sheng, Z., Sobieszczyk, M.E., et al. (2023). Changes in serum-neutralizing antibody potency and breadth post-SARS-CoV-2 mRNA vaccine boost. iScience *26*, 106345. https://doi.org/10.1016/j.isci.2023.106345.

70. Muecksch, F., Wang, Z., Cho, A., Gaebler, C., Ben Tanfous, T., DaSilva, J., Bednarski, E., Ramos, V., Zong, S., Johnson, B., et al. (2022). Increased memory B cell potency and breadth after a SARS-CoV-2 mRNA boost. Nature *607*, 128–134. https://doi.org/10.1038/s41586-022-04778-y.

71. Van Beek, M., Nussenzweig, M.C., and Chakraborty, A.K. (2022). Two complementary features of humoral immune memory confer protection against the same or variant antigens. Proc. Natl. Acad. Sci. *119*, e2205598119. https://doi.org/10.1073/pnas.2205598119.

72. Madhi, S.A., Kwatra, G., Myers, J.E., Jassat, W., Dhar, N., Mukendi, C.K., Nana, A.J., Blumberg, L., Welch, R., Ngorima-Mabhena, N., and Mutevedzi, P.C. (2022). Population Immunity and Covid-19 Severity with Omicron Variant in South Africa. N. Engl. J. Med. *386*, 1314–1326. https://doi.org/10.1056/NEJMoa2119658.

73. Goodman, B. (2022). Quick and Stealthy New Covid-19 Variants Are Poised to Drive a Winter Surge (CNN). https://www.cnn.com/2022/10/20/health/variants-covid-winter-surge/index.html.

74. (2023). WHO Elevates XBB.1.16 to Variant of Interest as Levels Rise in US and Other Countries | CIDRAP. https://www.cidrap.umn.edu/covid-19/who-elevates-xbb116-variant-interest-levels-rise-us-and-other-countries.

75. Dadonaite, B., Crawford, K.H.D., Radford, C.E., Farrell, A.G., Yu, T.C., Hannon, W.W., Zhou, P., Andrabi, R., Burton, D.R., Liu, L., et al. (2023). A pseudovirus system enables deep mutational scanning of the full SARS-CoV-2 spike. Cell *186*, 1263–1278.e20. https://doi.org/10.1016/j.cell.2023.02.001.

76. Mondeali, M., Etemadi, A., Barkhordari, K., Mobini Kesheh, M., Shavandi, S., Bahavar, A., Tabatabaie, F.H., Mahmoudi Gomari, M., and Modarressi, M.H. (2023). The role of S477N mutation in the molecular behavior of SARS-CoV-2 spike protein: An in-silico perspective. J. Cell. Biochem. *124*, 308–319. https://doi.org/10.1002/jcb.30367.

77. Singh, A., Steinkellner, G., Köchl, K., Gruber, K., and Gruber, C.C. (2021). Serine 477 plays a crucial role in the interaction of the SARS-CoV-2 spike protein with the human receptor ACE2. Sci. Rep. *11*, 4320. https://doi.org/10.1038/s41598-021-83761-5.

78. Zhang, L., Jackson, C.B., Mou, H., Ojha, A., Peng, H., Quinlan, B.D., Rangarajan, E.S., Pan, A., Vanderheiden, A., Suthar, M.S., et al. (2020). SARS-CoV-2 spike-protein D614G mutation increases virion spike density and infectivity. Nat. Commun. *11*, 6013. https://doi.org/10.1038/s41467-020-19808-4.

79. Chalkias, S., Harper, C., Vrbicky, K., Walsh, S.R., Essink, B., Brosz, A., McGhee, N., Tomassini, J.E., Chen, X., Chang, Y., et al. (2022). A Bivalent Omicron-Containing Booster Vaccine against Covid-19. N. Engl. J. Med. *387*, 1279–1291.

80. Lasrado, N., Collier, A.R.Y., Miller, J., Hachmann, N.P., Liu, J., Sciacca, M., Wu, C., Anand, T., Bondzie, E.A., Fisher, J.L., et al. (2023). Waning Immunity Against XBB.1.5 Following Bivalent mRNA Boosters. bioRxiv *2023*, 2023.01.22.525079. https://doi.org/10.1101/2023.01.22.525079.

81. Lin, D.-Y., Xu, Y., Gu, Y., Zeng, D., Sunny, S.K., and Moore, Z. (2023). Durability of Bivalent Boosters against Omicron Subvariants. N. Engl. J. Med. *388*, 1818–1820. https://doi.org/10.1056/NEJMc2302462.

82. U.S. CDC and Advisory Committee Recommend Use of Authorized and Approved 2023-2024 Monovalent XBB COVID-19 Vaccines - Sep 12, 2023 https://ir.novavax.com/press-releases/US-CDC-and-Advisory-Committee-Recommend-Use-of-Authorized-and-Approved-2023-2024-Monovalent-XBB-COVID-19-Vaccines.

83. Commissioner (2023). FDA Takes Action on Updated mRNA COVID-19 Vaccines to Better Protect against Currently Circulating Variants (FDA). https://www.fda.gov/news-events/press-announcements/fda-takes-action-updated-mrna-covid-19-vaccines-better-protect-against-currently-circulating.

84. Ozono, S., Zhang, Y., Ode, H., Sano, K., Tan, T.S., Imai, K., Miyoshi, K., Kishigami, S., Ueno, T., Iwatani, Y., et al. (2021). SARS-CoV-2 D614G spike mutation increases entry efficiency with enhanced ACE2-binding affinity. Nat. Commun. *12*, 848. https://doi.org/10.1038/s41467-021-21118-2.

85. Yurkovetskiy, L., Egri, S., Kurhade, C., Diaz-Salinas, M.A., Jaimes, J.A., Nyalile, T., Xie, X., Choudhary, M.C., Dauphin, A., Li, J.Z., et al. (2023). S:D614G and S:H655Y are gateway mutations that act epistatically to promote SARS-CoV-2 variant fitness. Preprint at bioRxiv. https://doi.org/10.1101/2023.03.30.535005.

86. Tian, F., Tong, B., Sun, L., Shi, S., Zheng, B., Wang, Z., Dong, X., and Zheng, P. (2021). N501Y mutation of spike protein in SARS-CoV-2 strengthens its binding to receptor ACE2. Elife *10*, e69091. https://doi.org/10.7554/eLife.69091.

87. Barton, M.I., MacGowan, S.A., Kutuzov, M.A., Dushek, O., Barton, G.J., and van der Merwe, P.A. (2021). Effects of common mutations in the SARS-CoV-2 Spike RBD and its ligand, the human ACE2 receptor on binding affinity and kinetics. Elife *10*, e70658. https://doi.org/10.7554/eLife.70658.

88. Mungmunpuntipantip, R., and Wiwanitkit, V. (2022). Change in binding affinity with ACE2 receptor in beta, delta and omicron SARS CoV2 variants. Int. J. Physiol. Pathophysiol. Pharmacol. *14*, 124–128.

89. Li, L., Liao, H., Meng, Y., Li, W., Han, P., Liu, K., Wang, Q., Li, D., Zhang, Y., Wang, L., et al. (2022). Structural basis of human ACE2 higher binding affinity to currently circulating Omicron SARS-CoV-2 sub-variants BA.2 and BA.1.1. Cell *185*, 2952–2960.e10. https://doi.org/10.1016/j.cell.2022.06.023.

90. Wang, Y., Liu, C., Zhang, C., Wang, Y., Hong, Q., Xu, S., Li, Z., Yang, Y., Huang, Z., and Cong, Y. (2022). Structural basis for SARS-CoV-2 Delta variant recognition of ACE2 receptor and broadly neutralizing antibodies. Nat. Commun. *13*, 871. https://doi.org/10.1038/s41467-022-28528-w.

91. Link-Gelles, R., Ciesla, A.A., Roper, L.E., Scobie, H.M., Ali, A.R., Miller, J.D., Wiegand, R.E., Accorsi, E.K., Verani, J.R., Shang, N., et al. (2023). Early Estimates of Bivalent mRNA Booster Dose Vaccine Effectiveness in Preventing Symptomatic SARS-CoV-2 Infection Attributable to Omicron BA.5– and XBB/XBB.1.5–Related Sublineages Among Immunocompetent Adults — Increasing Community Access to Testing Program, United States, December 2022–January 2023. MMWR Morb. Mortal. Wkly. Rep. *72*, 119–124. https://doi.org/10.15585/mmwr.mm7205e1.

92. Tartof, S.Y., Slezak, J.M., Puzniak, L., Hong, V., Frankland, T.B., Ackerson, B.K., Xie, F., Takhar, H., Ogun, O.A., Simmons, S., et al. (2023). Effectiveness of BNT162b2 BA.4/5 bivalent mRNA vaccine against a range of COVID-19 outcomes in a large health system in the USA: a test-negative case–control study. Lancet Respir. Med. *11*, 1089–1100. https://doi.org/10.1016/S2213-2600(23)00306-5.

93. Dacon, C., Peng, L., Lin, T.-H., Tucker, C., Lee, C.-C.D., Cong, Y., Wang, L., Purser, L., Cooper, A.J.R., Williams, J.K., et al. (2023). Rare, convergent antibodies targeting the stem helix broadly neutralize diverse betacoronaviruses. Cell Host Microbe *31*, 97–111.e12. https://doi.org/10.1016/j.chom.2022.10.010.

94. Wang, C., van Haperen, R., Gutiérrez-Álvarez, J., Li, W., Okba, N.M.A., Albulescu, I., Widjaja, I., van Dieren, B., Fernandez-Delgado, R., Sola, I., et al. (2021). A conserved immunogenic and vulnerable site on the coronavirus spike protein delineated by cross-reactive monoclonal antibodies. Nat. Commun. *12*, 1715. https://doi.org/10.1038/s41467-021-21968-w.

95. Zhou, P., Song, G., Liu, H., Yuan, M., He, W.T., Beutler, N., Zhu, X., Tse, L.V., Martinez, D.R., Schäfer, A., et al. (2023). Broadly neutralizing anti-S2 antibodies protect against all three human betacoronaviruses that cause deadly disease. Immunity *56*, 669–686.e7. https://doi.org/10.1016/j.immuni.2023.02.005.

96. Pinto, D., Sauer, M.M., Czudnochowski, N., Low, J.S., Tortorici, M.A., Housley, M.P., Noack, J., Walls, A.C., Bowen, J.E., Guarino, B., et al. (2021). Broad betacoronavirus neutralization by a stem helix–specific human antibody. Science *373*, 1109–1116. https://doi.org/10.1126/science.abj3321.

97. Low, J.S., Jerak, J., Tortorici, M.A., McCallum, M., Pinto, D., Cassotta, A., Foglierini, M., Mele, F., Abdelnabi, R., Weynand, B., et al. (2022). ACE2-binding exposes the SARS-CoV-2 fusion peptide to broadly neutralizing coronavirus antibodies. Science *377*, 735–742. https://doi.org/10.1126/science.abq2679.

98. Sun, X., Yi, C., Zhu, Y., Ding, L., Xia, S., Chen, X., Liu, M., Gu, C., Lu, X., Fu, Y., et al. (2022). Neutralization mechanism of a human antibody with pan-coronavirus reactivity including SARS-CoV-2. Nat. Microbiol. *7*, 1063–1074. https://doi.org/10.1038/s41564-022-01155-3.

99. Dacon, C., Tucker, C., Peng, L., Lee, C.-C.D., Lin, T.-H., Yuan, M., Cong, Y., Wang, L., Purser, L., Williams, J.K., et al. (2022). Broadly neutralizing antibodies target the coronavirus fusion peptide. Science *377*, 728–735. https://doi.org/10.1126/science.abq3773.

100. Bianchini, F., Crivelli, V., Abernathy, M.E., Guerra, C., Palus, M., Muri, J., Marcotte, H., Piralla, A., Pedotti, M., De Gasparo, R., et al. (2023). Human neutralizing antibodies to cold linear epitopes and subdomain 1 of the SARS-CoV-2 spike glycoprotein. Sci. Immunol. *8*, eade0958. https://doi.org/10.1126/sciimmunol.ade0958.

101. Canaday, D.H., Oyebanji, O.A., Keresztesy, D., Payne, M., Wilk, D., Carias, L., Aung, H., St. Denis, K., Lam, E.C., Rowley, C.F., et al. (2022). Significant Reduction in Vaccine-Induced Antibody Levels and Neutralization Activity Among Healthcare Workers and Nursing Home Residents 6 Months Following Coronavirus Disease 2019 BNT162b2 mRNA Vaccination. Clin. Infect. Dis. *75*, e884–e887. https://doi.org/10.1093/cid/ciab963.

102. Canaday, D.H., Oyebanji, O.A., White, E., Keresztesy, D., Payne, M., Wilk, D., Carias, L., Aung, H., St. Denis, K., Sheehan, M.L., et al. (2022). COVID-19 vaccine booster dose needed to achieve Omicron-specific neutralisation in nursing home residents. EBioMedicine *80*, 104066. https://doi.org/10.1016/j.ebiom.2022.104066.

103. Siebring-van Olst, E., Vermeulen, C., de Menezes, R.X., Howell, M., Smit, E.F., and van Beusechem, V.W. (2013). Affordable luciferase reporter assay for cell-based high-throughput screening. J Biomol. Screen. *18*, 453–461. https://doi.org/10.1177/1087057112465184.

STAR★METHODS

KEY RESOURCES TABLE

REAGENT or RESOURCE	SOURCE	IDENTIFIER
Bacterial and virus strains		
DH5α Zymo-Competent *E. coli*	Zymo	Cat# T3009
Chemicals, peptides, and recombinant proteins		
Phosphate buffered saline (PBS)	Corning	Cat# 21-031-CV
Dulbecco's modified eagle medium (DMEM)	Corning	Cat# 10-013-CV
Fetal bovine serum (FBS)	VWR	Cat# 89510-186
Paraformaldehyde Solution, 4% in PBS, Affymetrix/USB™	Fisher Scientific	Cat# AAJ19943K2
Penicillin/streptomycin	Corning	Cat# 30-002-CI
Polyethylenimine 25K MW, linear	Polysciences Inc	Cat# 23966
Puromycin	Sigma	Cat# P8833-10MG
ATP	Sigma	Cat# A2383-5G
Magnesium chloride	BDH	Cat# BDH9244-500G
Magnesium sulfate	BDH	Cat# BDH9246-500G
Dithiothreitol (DTT)	VWR	Cat# 97061-338
D-luciferin	Gold Bio	Cat# LUCK-2G
EDTA	Sigma	Cat# 03690-100ML
Triton X-100	Fisher	Cat# BP151-500
Polybrene	Sigma	Cat# H9268-5G
qScript XLT 1-Step RT-qPCR ToughMix, Low-ROX	Quantabio	Cat# 95134-500
Turbo DNase	Fisher	Cat# AM2239
Recombinant Human ACE-2 His-tag Alexa Fluor® 647 Protein	R&D Systems	Cat# AFR933
Experimental models: Cell lines		
HEK293T/17 Cells	ATCC	Cat# CRL-11268
293T/ACE2.MF	Obtained from the lab of Dr. Michael Farzan	N/A
Oligonucleotides		
Lentivirus LTR qPCR Probe/56-FAM/ AGC+C/i5NitInd/GG + GA/ZEN/GCT CTCTGGC/3IABkFQ/	Integrated DNA Technology	N/A
Lentivirus LTR qPCR 5′ Primer GGTCTCTCTIGITAGACCAG	Integrated DNA Technology	N/A
Lentivirus LTR qPCR 3′ Primer TTTATTGAGGCTTAAGCAGTGGG	Integrated DNA Technology	N/A
Recombinant DNA		
pHAGE-CMV-Luc2-IRES-ZsGreen-W (backbone)	This study	Addgene Plasmid ID 164432
pTwist-SARS-CoV-2 Δ18 (spike)	This study	Addgene Plasmid ID 164436
pTwist-SARS-CoV-2 Δ18 B.1.617.2v1 (spike)	This study	Addgene Plasmid ID 179905
pTwist-SARS-CoV-2 Δ18 B.1.351v2 (spike)	This study	Addgene Plasmid ID 169463
pTwist-SARS-CoV-2 Δ18 P.1 (spike)	This study	Addgene Plasmid ID 173476
pTwist-SARS-CoV-2 Δ18 B.1.1.529 (spike)	This study	Addgene Plasmid ID 179906
pTwist-SARS-CoV-2 Spike-ΔC18 A222V (GTG)	This study	Addgene Plasmid ID 212329
pTwist-SARS-CoV-2 Spike-ΔC18 D253G (GGC)	This study	Addgene Plasmid ID 212330

(*Continued on next page*)

Continued

REAGENT or RESOURCE	SOURCE	IDENTIFIER
pTwist-SARS-CoV-2 Spike-ΔC18 E281V (GTA)	This study	Addgene Plasmid ID 212331
pTwist-SARS-CoV-2 Spike-ΔC18 N439K (AAA)	This study	Addgene Plasmid ID 212332
pTwist-SARS-CoV-2 Spike-ΔC18 S477N (AAC)	This study	Addgene Plasmid ID 212333
pTwist-SARS-CoV-2 Spike-ΔC18 D936Y (TAT)	This study	Addgene Plasmid ID 212334
pTwist-SARS-CoV-2 Spike-ΔC18 L5F (TTC)	This study	Addgene Plasmid ID 212335
pTwist-SARS-CoV-2 Spike-ΔC18 ΔH69V70	This study	Addgene Plasmid ID 212336
pTwist-SARS-CoV-2 Spike-ΔC18 ΔY145	This study	Addgene Plasmid ID 212337
pTwist-SARS-CoV-2 Spike-ΔC18 N501Y (TAT)	This study	Addgene Plasmid ID 212338
pTwist-SARS-CoV-2 Spike-ΔC18 A570D (GAC)	This study	Addgene Plasmid ID 212339
pTwist-SARS-CoV-2 Spike-ΔC18 P681H (CAC)	This study	Addgene Plasmid ID 212340
pTwist-SARS-CoV-2 Spike-ΔC18 T716I (ATT)	This study	Addgene Plasmid ID 212341
pTwist-SARS-CoV-2 Spike-ΔC18 S982A (GCC)	This study	Addgene Plasmid ID 212342
pTwist-SARS-CoV-2 Spike-ΔC18 D1118H (CAC)	This study	Addgene Plasmid ID 212343
pTwist-SARS-CoV-2 Spike-ΔC18 D80A (GCT)	This study	Addgene Plasmid ID 212344
pTwist-SARS-CoV-2 Spike-ΔC18 D215G (GGT)	This study	Addgene Plasmid ID 212345
pTwist-SARS-CoV-2 Spike-ΔC18 L242H (CAT)	This study	Addgene Plasmid ID 212346
pTwist-SARS-CoV-2 Spike-ΔC18 K417N (AAT)	This study	Addgene Plasmid ID 212347
pTwist-SARS-CoV-2 Spike-ΔC18 E484K (AAA)	This study	Addgene Plasmid ID 212348
pTwist-SARS-CoV-2 Spike-ΔC18 A701V (GTT)	This study	Addgene Plasmid ID 212349
pTwist-SARS-CoV-2 Spike-ΔC18 SAK005321 (Wrong L242H)	This study	Addgene Plasmid ID 212350
pTwist-SARS-CoV-2 Spike-ΔC18 V1176F (TTC)	This study	Addgene Plasmid ID 212351
pTwist-SARS-CoV-2 Spike-ΔC18 K417N (AAT) E484K (AAA)	This study	Addgene Plasmid ID 212352
pTwist-SARS-CoV-2 Spike-ΔC18 K417N (AAT) N501Y (TAT)	This study	Addgene Plasmid ID 212353
pTwist-SARS-CoV-2 Spike-ΔC18 E484K (AAA) N501Y (TAT)	This study	Addgene Plasmid ID 212354
pTwist-SARS-CoV-2 Spike-ΔC18 ΔL242-L244	This study	Addgene Plasmid ID 212355
pTwist-SARS-CoV-2 Spike-ΔC18 R246I (ATA)	This study	Addgene Plasmid ID 212356
pTwist-SARS-CoV-2 Spike-ΔC18 ΔL242-L244 + R246I (ATA)	This study	Addgene Plasmid ID 212357
pTwist-SARS-CoV-2 Spike-ΔC18 L18F (TTC)	This study	Addgene Plasmid ID 212358
pTwist-SARS-CoV-2 Spike-ΔC18 T20N (AAT)	This study	Addgene Plasmid ID 212359
pTwist-SARS-CoV-2 Spike-ΔC18 P26S (TCC)	This study	Addgene Plasmid ID 212360
pTwist-SARS-CoV-2 Spike-ΔC18 D138Y (TAT)	This study	Addgene Plasmid ID 212361
pTwist-SARS-CoV-2 Spike-ΔC18 R190S (AGC)	This study	Addgene Plasmid ID 212362
pTwist-SARS-CoV-2 Spike-ΔC18 K417T (ACG)	This study	Addgene Plasmid ID 212363
pTwist-SARS-CoV-2 Spike-ΔC18 H655Y (TAT)	This study	Addgene Plasmid ID 212364
pTwist-SARS-CoV-2 Spike-ΔC18 T1027I (ATT)	This study	Addgene Plasmid ID 212365
pTwist-SARS-CoV-2 Spike-ΔC18 S13I (ATC)	This study	Addgene Plasmid ID 212366
2971 - pTwist-SARS-CoV-2 Spike-ΔC18 W152C (TGC)	This study	Addgene Plasmid ID 212367
pTwist-SARS-CoV-2 Spike-ΔC18 L452R (CGT)	This study	Addgene Plasmid ID 212368
pTwist-SARS-CoV-2 Spike-ΔC18 Y453F (TTC)	This study	Addgene Plasmid ID 212369
pTwist-SARS-CoV-2 Spike-ΔC18 I692V (GTA)	This study	Addgene Plasmid ID 212370
pTwist-SARS-CoV-2 Spike-ΔC18 M1229I (ATC)	This study	Addgene Plasmid ID 212371
pTwist-SARS-CoV-2 Spike-ΔC18 Danish Mink ΔFVI	This study	Addgene Plasmid ID 212372
pTwist-SARS-CoV-2 Spike-ΔC18 T307I (ATA)	This study	Addgene Plasmid ID 212373
pTwist-SARS-CoV-2 Spike-ΔC18 T572I (ATC)	This study	Addgene Plasmid ID 212374

(*Continued on next page*)

Continued

REAGENT or RESOURCE	SOURCE	IDENTIFIER
pTwist-SARS-CoV-2 Spike-ΔC18 Q239R (CGA)	This study	Addgene Plasmid ID 212375
pTwist-SARS-CoV-2 Spike-ΔC18 Q677H (CAT)	This study	Addgene Plasmid ID 212376
pTwist-SARS-CoV-2 Spike-ΔC18 T307I (ATA) T572I (ATC) D614G (GGT)	This study	Addgene Plasmid ID 212377
pTwist-SARS-CoV-2 Spike-ΔC18 Q239R (CGA) D614G (GGT)	This study	Addgene Plasmid ID 212378
pTwist-SARS-CoV-2 Spike-ΔC18 D614G (GGT) Q677H (CAT) D936Y (TAT)	This study	Addgene Plasmid ID 212379
pTwist-SARS-CoV-2 Spike-ΔC18 SAK006840 VOC-501Y.V2 (B.1.351v3) - No RBD Mutations	This study	Addgene Plasmid ID 212380
pTwist-SARS-CoV-2 Spike-ΔC18 VOC-501Y.V2 (B.1.351) - All Mutations	This study	Addgene Plasmid ID 212381
pTwist-SARS-CoV-2 Spike-ΔC18 K417T (ACG) E484K (AAA)	This study	Addgene Plasmid ID 212382
pTwist-SARS-CoV-2 Spike-ΔC18 K417T (ACG) N501Y (TAT)	This study	Addgene Plasmid ID 212383
pTwist-SARS-CoV-2 Spike-ΔC18 (P.1) - No RBD Mutations	This study	Addgene Plasmid ID 212384
pTwist-SARS-CoV-2 Spike-ΔC18 (P.2/B.1.1.248) - No RBD Mutations	This study	Addgene Plasmid ID 212385
pTwist-SARS-CoV-2 Spike-ΔC18 R683G (GGC)	This study	Addgene Plasmid ID 212386
pTwist-SARS-CoV-2 Spike-ΔC18 SA501.V2 (Triple RBD) R683G (GGC)	This study	Addgene Plasmid ID 212387
pTwist-SARS-CoV-2 Spike-ΔC18 VOC-501Y.V2 (B.1.351) - McGuire Mutations	This study	Addgene Plasmid ID 212388
pTwist-SARS-CoV-2 Spike-ΔC18 SA190 VOC-501Y.V2 (B.1.351v4)	This study	Addgene Plasmid ID 212389
pTwist-SARS-CoV-2 Spike-ΔC18 D215H (CAT)	This study	Addgene Plasmid ID 212390
pTwist-SARS-CoV-2 Spike-ΔC18 SAK006879 VOC-501Y.V2 (B.1.351v5)	This study	Addgene Plasmid ID 212391
pTwist-SARS-CoV-2 Spike-ΔC18 A27S (TCT)	This study	Addgene Plasmid ID 212392
pTwist-SARS-CoV-2 Spike-ΔC18 SAK007134 VOC-501Y.V2 (B.1.351v6)	This study	Addgene Plasmid ID 212393
pTwist-SARS-CoV-2 Spike-ΔC18 Q52R (CGA)	This study	Addgene Plasmid ID 212394
pTwist-SARS-CoV-2 Spike-ΔC18 A67V (GTT)	This study	Addgene Plasmid ID 212395
pTwist-SARS-CoV-2 Spike-ΔC18 A67V (GTT) + ΔH69V70	This study	Addgene Plasmid ID 212396
pTwist-SARS-CoV-2 Spike-ΔC18 F888L (CTT)	This study	Addgene Plasmid ID 212397
pTwist-SARS-CoV-2 Spike-ΔC18 (B.1.525)	This study	Addgene Plasmid ID 212398
pTwist-SARS-CoV-2 Spike-ΔC18 (Robin)	This study	Addgene Plasmid ID 212399
pTwist-SARS-CoV-2 Spike-ΔC18 Q677P (CCA)	This study	Addgene Plasmid ID 212400
pTwist-SARS-CoV-2 Spike-ΔC18 (Pelican)	This study	Addgene Plasmid ID 212401
pTwist-SARS-CoV-2 Spike-ΔC18 (Yellowhammer)	This study	Addgene Plasmid ID 212402
pTwist-SARS-CoV-2 Spike-ΔC18 T29I (ATA)	This study	Addgene Plasmid ID 212403
pTwist-SARS-CoV-2 Spike-ΔC18 T572I (ATC)	This study	Addgene Plasmid ID 212404
pTwist-SARS-CoV-2 Spike-ΔC18 D936N (AAT)	This study	Addgene Plasmid ID 212405
pTwist-SARS-CoV-2 Spike-ΔC18 (Bluebird)	This study	Addgene Plasmid ID 212406
pTwist-SARS-CoV-2 Spike-ΔC18 T732S (AGT)	This study	Addgene Plasmid ID 212407
pTwist-SARS-CoV-2 Spike-ΔC18 (Quail)	This study	Addgene Plasmid ID 212408
pTwist-SARS-CoV-2 Spike-ΔC18 G142S (AGC)	This study	Addgene Plasmid ID 212409
pTwist-SARS-CoV-2 Spike-ΔC18 E180V (GTA)	This study	Addgene Plasmid ID 212410

(*Continued on next page*)

Continued

REAGENT or RESOURCE	SOURCE	IDENTIFIER
pTwist-SARS-CoV-2 Spike-ΔC18 (Mockingbird)	This study	Addgene Plasmid ID 212411
pTwist-SARS-CoV-2 Spike-ΔC18 (P.1) Triple RBD	This study	Addgene Plasmid ID 212412
pTwist-SARS-CoV-2 Spike-ΔC18 T95I (ATA)	This study	Addgene Plasmid ID 212413
pTwist-SARS-CoV-2 Spike-ΔC18 Q957R (CGG)	This study	Addgene Plasmid ID 212414
pTwist-SARS-CoV-2 Spike-ΔC18 B.1.526v1	This study	Addgene Plasmid ID 212415
pTwist-SARS-CoV-2 Spike-ΔC18 B.1.526v2	This study	Addgene Plasmid ID 212416
pTwist-SARS-CoV-2 Spike-ΔC18 T19R (AGA)	This study	Addgene Plasmid ID 212417
pTwist-SARS-CoV-2 Spike-ΔC18 K77T (ACG)	This study	Addgene Plasmid ID 212418
pTwist-SARS-CoV-2 Spike-ΔC18 G142D (GAT)	This study	Addgene Plasmid ID 212419
pTwist-SARS-CoV-2 Spike-ΔC18 E154K (AAA)	This study	Addgene Plasmid ID 212420
pTwist-SARS-CoV-2 Spike-ΔC18 ΔE156-F157 + R158G (GGA)	This study	Addgene Plasmid ID 212421
pTwist-SARS-CoV-2 Spike-ΔC18 T478K (AAA)	This study	Addgene Plasmid ID 212422
pTwist-SARS-CoV-2 Spike-ΔC18 E484Q (CAA)	This study	Addgene Plasmid ID 212423
pTwist-SARS-CoV-2 Spike-ΔC18 P681R (CGT)	This study	Addgene Plasmid ID 212424
pTwist-SARS-CoV-2 Spike-ΔC18 D950N (AAT)	This study	Addgene Plasmid ID 212425
pTwist-SARS-CoV-2 Spike-ΔC18 Q1071H (CAT)	This study	Addgene Plasmid ID 212426
pTwist-SARS-CoV-2 Spike-ΔC18 H1101D (GAC)	This study	Addgene Plasmid ID 212427
pTwist-SARS-CoV-2 Spike-ΔC18 B.1.617v1 (B.1.617.1 v1)	This study	Addgene Plasmid ID 212428
pTwist-SARS-CoV-2 Spike-ΔC18 B.1.617v2 (B.1.617.1 v2)	This study	Addgene Plasmid ID 212429
pTwist-SARS-CoV-2 Spike-ΔC18 B.1.617v3 (B.1.617.2 v2)	This study	Addgene Plasmid ID 212430
pTwist-SARS-CoV-2 Spike-ΔC18 B.1.617v4 (B.1.617.2 v1)	This study	Addgene Plasmid ID 212431
pTwist-SARS-CoV-2 Spike-ΔC18 V70F (TTT)	This study	Addgene Plasmid ID 212432
pTwist-SARS-CoV-2 Spike-ΔC18 W258L (CTG)	This study	Addgene Plasmid ID 212433
pTwist-SARS-CoV-2 Spike-ΔC18 AY.1	This study	Addgene Plasmid ID 212434
pTwist-SARS-CoV-2 Spike-ΔC18 AY.2	This study	Addgene Plasmid ID 212435
pTwist-SARS-CoV-2 Spike-ΔC18 K417N (AAT) L452R (CGT)	This study	Addgene Plasmid ID 212436
pTwist-SARS-CoV-2 Spike-ΔC18 K417N (AAT) T478K (AAA)	This study	Addgene Plasmid ID 212437
pTwist-SARS-CoV-2 Spike-ΔC18 L452R (CGT) T478K (AAA)	This study	Addgene Plasmid ID 212438
pTwist-SARS-CoV-2 Spike-ΔC18 K417N (AAT) L452R (CGT) T478K (AAA)	This study	Addgene Plasmid ID 212439
pTwist-SARS-CoV-2 Spike-ΔC18 K417N (AAT) L452R (CGT) T478K (AAA) E484K (AAA)	This study	Addgene Plasmid ID 212440
pTwist-SARS-CoV-2 Spike-ΔC18 K417N (AAT) L452R (CGT) T478K (AAA) E484Q (CAA)	This study	Addgene Plasmid ID 212441
pTwist-SARS-CoV-2 Spike-ΔC18 G75V (GTA)	This study	Addgene Plasmid ID 212442
pTwist-SARS-CoV-2 Spike-ΔC18 T76I (ATT)	This study	Addgene Plasmid ID 212443
pTwist-SARS-CoV-2 Spike-ΔC18 G75V (GTA) T76I (ATT)	This study	Addgene Plasmid ID 212444
pTwist-SARS-CoV-2 Spike-ΔC18 ΔR246-G252 + D253N (AAC)	This study	Addgene Plasmid ID 212445
pTwist-SARS-CoV-2 Spike-ΔC18 L452Q (CAA)	This study	Addgene Plasmid ID 212446
pTwist-SARS-CoV-2 Spike-ΔC18 F490S (TCT)	This study	Addgene Plasmid ID 212447
pTwist-SARS-CoV-2 Spike-ΔC18 T859N (AAC)	This study	Addgene Plasmid ID 212448
pTwist-SARS-CoV-2 Spike-ΔC18 C.37	This study	Addgene Plasmid ID 212449
pTwist-SARS-CoV-2 Spike-ΔC18 L452Q (CAA) F490S (TCT)	This study	Addgene Plasmid ID 212450

(*Continued on next page*)

Continued

REAGENT or RESOURCE	SOURCE	IDENTIFIER
pTwist-SARS-CoV-2 Spike-ΔC18 YY144TSN (ACTTCTAAC)	This study	Addgene Plasmid ID 212451
pTwist-SARS-CoV-2 Spike-ΔC18 R346K (AAA)	This study	Addgene Plasmid ID 212452
pTwist-SARS-CoV-2 Spike-ΔC18 B.1.621 (Mu)	This study	Addgene Plasmid ID 212453
pTwist-SARS-CoV-2 Spike-ΔC18 G339H	This study	Addgene Plasmid ID 212454
pTwist-SARS-CoV-2 Spike-ΔC18 EG.5.1	This study	Addgene Plasmid ID 212455
pTwist-SARS-CoV-2 Spike-ΔC18 Y145H (CAT)	This study	Addgene Plasmid ID 212456
pTwist-SARS-CoV-2 Spike-ΔC18 AY.4.2	This study	Addgene Plasmid ID 212457
pTwist-SARS-CoV-2 Spike-ΔC18 ΔV143-Y145	This study	Addgene Plasmid ID 212458
pTwist-SARS-CoV-2 Spike-ΔC18 G142D (GAT)+ΔV143-Y145	This study	Addgene Plasmid ID 212459
pTwist-SARS-CoV-2 Spike-ΔC18 N211I (ATT)+ΔL212	This study	Addgene Plasmid ID 212460
pTwist-SARS-CoV-2 Spike-ΔC18 InsertionR214-EPE	This study	Addgene Plasmid ID 212461
pTwist-SARS-CoV-2 Spike-ΔC18 N211I (ATT) ΔL212+InsertionR214-EPE	This study	Addgene Plasmid ID 212462
pTwist-SARS-CoV-2 Spike-ΔC18 G339D (GAT)	This study	Addgene Plasmid ID 212463
pTwist-SARS-CoV-2 Spike-ΔC18 S371L (CTC)	This study	Addgene Plasmid ID 212464
pTwist-SARS-CoV-2 Spike-ΔC18 S373P (CCA)	This study	Addgene Plasmid ID 212465
pTwist-SARS-CoV-2 Spike-ΔC18 S375F (TTC)	This study	Addgene Plasmid ID 212466
pTwist-SARS-CoV-2 Spike-ΔC18 S371L (CTC) S373P (CCA) S375F (TTC)	This study	Addgene Plasmid ID 212467
pTwist-SARS-CoV-2 Spike-ΔC18 G446S (AGC)	This study	Addgene Plasmid ID 212468
pTwist-SARS-CoV-2 Spike-ΔC18 N440K (AAG) G446S (AGC)	This study	Addgene Plasmid ID 212469
pTwist-SARS-CoV-2 Spike-ΔC18 S477N (AAC) T478K (AAA)	This study	Addgene Plasmid ID 212470
pTwist-SARS-CoV-2 Spike-ΔC18 E484A (GCA)	This study	Addgene Plasmid ID 212471
pTwist-SARS-CoV-2 Spike-ΔC18 S477N (AAC) T478K (AAA) E484A (GCA)	This study	Addgene Plasmid ID 212472
pTwist-SARS-CoV-2 Spike-ΔC18 Q493R (CGA)	This study	Addgene Plasmid ID 212473
pTwist-SARS-CoV-2 Spike-ΔC18 G496S (TCA)	This study	Addgene Plasmid ID 212474
pTwist-SARS-CoV-2 Spike-ΔC18 Q498R (CGA)	This study	Addgene Plasmid ID 212475
pTwist-SARS-CoV-2 Spike-ΔC18 Y505H (CAT)	This study	Addgene Plasmid ID 212476
pTwist-SARS-CoV-2 Spike-ΔC18 Q493R (CGA) G496S (TCA) Q498R (CGA) N501Y (TAT) Y505H (CAT)	This study	Addgene Plasmid ID 212477
pTwist-SARS-CoV-2 Spike-ΔC18 T547K (AAA)	This study	Addgene Plasmid ID 212478
pTwist-SARS-CoV-2 Spike-ΔC18 N679K (AAA)	This study	Addgene Plasmid ID 212479
pTwist-SARS-CoV-2 Spike-ΔC18 N679K (AAA) P681H (CAC)	This study	Addgene Plasmid ID 212480
pTwist-SARS-CoV-2 Spike-ΔC18 N764K (AAA)	This study	Addgene Plasmid ID 212481
pTwist-SARS-CoV-2 Spike-ΔC18 D796Y (TAT)	This study	Addgene Plasmid ID 212482
pTwist-SARS-CoV-2 Spike-ΔC18 N856K (AAG)	This study	Addgene Plasmid ID 212483
pTwist-SARS-CoV-2 Spike-ΔC18 Q954H (CAC)	This study	Addgene Plasmid ID 212484
pTwist-SARS-CoV-2 Spike-ΔC18 N969K (AAA)	This study	Addgene Plasmid ID 212485
pTwist-SARS-CoV-2 Spike-ΔC18 L981F (TTC)	This study	Addgene Plasmid ID 212486
pTwist-SARS-CoV-2 Spike-ΔC18 BA.2	This study	Addgene Plasmid ID 212487
pTwist-SARS-CoV-2 Spike-ΔC18 T19I (ATA)	This study	Addgene Plasmid ID 212488
pTwist-SARS-CoV-2 Spike-ΔC18 ΔL24P25P26 A27S (TCT)	This study	Addgene Plasmid ID 212489

(*Continued on next page*)

Continued

REAGENT or RESOURCE	SOURCE	IDENTIFIER
pTwist-SARS-CoV-2 Spike-ΔC18 V213G (GGT)	This study	Addgene Plasmid ID 212490
pTwist-SARS-CoV-2 Spike-ΔC18 S371F (TTC)	This study	Addgene Plasmid ID 212491
pTwist-SARS-CoV-2 Spike-ΔC18 T376A (GCT)	This study	Addgene Plasmid ID 212492
pTwist-SARS-CoV-2 Spike-ΔC18 S371F (TTC) S373P (CCA) S375F (TTC) T376A (GCT)	This study	Addgene Plasmid ID 212493
pTwist-SARS-CoV-2 Spike-ΔC18 D405N (AAC)	This study	Addgene Plasmid ID 212494
pTwist-SARS-CoV-2 Spike-ΔC18 R408S (AGC)	This study	Addgene Plasmid ID 212495
pTwist-SARS-CoV-2 Spike-ΔC18 D405N (AAC) R408S (AGC)	This study	Addgene Plasmid ID 212496
pTwist-SARS-CoV-2 Spike-ΔC18 N440K (AAG)	This study	Addgene Plasmid ID 212497
pTwist-SARS-CoV-2 Spike-ΔC18 Q493R (CGA) Q498R (CGA) N501Y (TAT) Y505H (CAT)	This study	Addgene Plasmid ID 212498
pTwist-SARS-CoV-2 Spike-ΔC18 Q954H (CAT)	This study	Addgene Plasmid ID 212499
pTwist-SARS-CoV-2 Spike-ΔC18 V3G (GGT)	This study	Addgene Plasmid ID 212500
pTwist-SARS-CoV-2 Spike-ΔC18 F486V (GTT)	This study	Addgene Plasmid ID 212501
pTwist-SARS-CoV-2 Spike-ΔC18 S704L (TTA)	This study	Addgene Plasmid ID 212502
pTwist-SARS-CoV-2 Spike-ΔC18 BA.2.12.1	This study	Addgene Plasmid ID 212503
pTwist-SARS-CoV-2 Spike-ΔC18 BA.4 + V3G	This study	Addgene Plasmid ID 212504
pTwist-SARS-CoV-2 Spike-ΔC18 BA.5	This study	Addgene Plasmid ID 212505
pTwist-SARS-CoV-2 Spike-ΔC18 BA.2.75	This study	Addgene Plasmid ID 212506
pTwist-SARS-CoV-2 Spike-ΔC18 BQ.1.1	This study	Addgene Plasmid ID 212507
pTwist-SARS-CoV-2 Spike-ΔC18 BA.2.75.2	This study	Addgene Plasmid ID 212508
pTwist-SARS-CoV-2 Spike-ΔC18 R346T(ACA)	This study	Addgene Plasmid ID 212509
pTwist-SARS-CoV-2 Spike-ΔC18 N460K(AAG)	This study	Addgene Plasmid ID 212510
pTwist-SARS-CoV-2 Spike-ΔC18 K444T(ACA)	This study	Addgene Plasmid ID 212511
pTwist-SARS-CoV-2 Spike-ΔC18 F486S(TCT)	This study	Addgene Plasmid ID 212512
pTwist-SARS-CoV-2 Spike-ΔC18 D1199N(AAC)	This study	Addgene Plasmid ID 212513
pTwist-SARS-CoV-2 Spike-ΔC18 W152R(CGG)	This study	Addgene Plasmid ID 212514
pTwist-SARS-CoV-2 Spike-ΔC18 F157L(TTA)	This study	Addgene Plasmid ID 212515
pTwist-SARS-CoV-2 Spike-ΔC18 K147E(GAG)	This study	Addgene Plasmid ID 212516
pTwist-SARS-CoV-2 Spike-ΔC18 I210V(GTA)	This study	Addgene Plasmid ID 212517
pTwist-SARS-CoV-2 Spike-ΔC18 G257S(AGT)	This study	Addgene Plasmid ID 212518
pTwist-SARS-CoV-2 Spike-ΔC18 BA.4	This study	Addgene Plasmid ID 212519
pTwist-SARS-CoV-2 Spike-ΔC18 BQ.1.1.22 (ΔY144)	This study	Addgene Plasmid ID 212520
pTwist-SARS-CoV-2 Spike-ΔC18 XBB	This study	Addgene Plasmid ID 212521
pTwist-SARS-CoV-2 Spike-ΔC18 XBB.1	This study	Addgene Plasmid ID 212522
pTwist-SARS-CoV-2 Spike-ΔC18 XBB.1.5	This study	Addgene Plasmid ID 212523
pTwist-SARS-CoV-2 Spike-ΔC18 V83A	This study	Addgene Plasmid ID 212524
pTwist-SARS-CoV-2 Spike-ΔC18 H146Q	This study	Addgene Plasmid ID 212525
pTwist-SARS-CoV-2 Spike-ΔC18 Q183E	This study	Addgene Plasmid ID 212526
pTwist-SARS-CoV-2 Spike-ΔC18 V213E	This study	Addgene Plasmid ID 212527
pTwist-SARS-CoV-2 Spike-ΔC18 G252V	This study	Addgene Plasmid ID 212528
pTwist-SARS-CoV-2 Spike-ΔC18 L368I	This study	Addgene Plasmid ID 212529
pTwist-SARS-CoV-2 Spike-ΔC18 V445P	This study	Addgene Plasmid ID 212530
pTwist-SARS-CoV-2 Spike-ΔC18 F486P	This study	Addgene Plasmid ID 212531
pTwist-SARS-CoV-2 Spike-ΔC18 XBB.1.16	This study	Addgene Plasmid ID 212532
pTwist-SARS-CoV-2 Spike-ΔC18 T478R (AGA)	This study	Addgene Plasmid ID 212533
pTwist-SARS-CoV-2 Spike-ΔC18 XBB.1 T478R	This study	Addgene Plasmid ID 212534

(*Continued on next page*)

Continued

REAGENT or RESOURCE	SOURCE	IDENTIFIER
pTwist-SARS-CoV-2 Spike-ΔC18 HK.3	This study	Addgene Plasmid ID 212572
pTwist-SARS-CoV-2 Spike-ΔC18 BA.2.86	This study	Addgene Plasmid ID 212538
pTwist-SARS-CoV-2 Spike-ΔC18 JN.1	This study	Addgene Plasmid ID 216526
pTwist-SARS-CoV-2 Spike-ΔC18 KP.2	This study	Addgene Plasmid ID 223273
pTwist-SARS-CoV-2 Spike-ΔC18 KP.3	This study	Addgene Plasmid ID 223276
pHDM-Hgpm2 (Gag-Pol)	This study	Addgene Plasmid ID 164441
pHDM-Tat1b (helper)	This study	Addgene Plasmid ID 164442
pRC-CMV-Rev1b (helper)	This study	Addgene Plasmid ID164443
Software and algorithms		
GraphPad Prism 9.4.158	Graphpad Software	www.graphpad.com/scientific-software/prism/; RRID:SCR_002798
Geneious Prime 2023	Geneious	http://www.geneious.com/; RRID:SCR_010519
FlowJo 10	FlowJo	https://www.flowjo.com; RRID:SCR_008520
Fluent Control	Tecan	https://lifesciences.tecan.com/fluent-laboratory-automation-workstation?p=tab–4
R v2023.06.1 + 524	Open source software	https://cran.r-project.org/bin/windows/base/; RRID:SCR_001905
CellCapTure	Stratedigm	https://stratedigm.com/cellcapture/
QuantStudio 12K Software v1.3	Applied Biosciences	https://www.thermofisher.com/us/en/home/global/forms/quantstudio-12k-flex-software-download.html

EXPERIMENTAL MODEL AND STUDY PARTICIPANT DETAILS

Human subjects

Use of human samples was approved by Partners Institutional Review Board (protocol 2020P002274) and the WCG Institutional Review Board (protocol 1316159). Serum samples from 42 vaccine recipients that received two or three doses of the BNT162b2 or mRNA-1273 vaccine were collected. For each individual, basic demographic information including age and gender as well as any relevant COVID-19 history was obtained. The current analysis is part of an ongoing study[101,102] in which 29 NH residents and 7 healthcare workers (HCWs) are consented directly or through their legally authorized representative if needed and serially sampled before and after each SARS-CoV-2 vaccine dose. This analysis includes data collected between August 23, 2021, and September 8, 2022. HCWs worked at 3 NH buildings, 2 Cleveland area hospitals, and Case Western Reserve University. Residents and HCWs who received SARS-CoV-2 mRNA vaccines [(BNT162b2 (Pfizer-BioNTech) or mRNA-1273 (Moderna)] were included, and those who received the Ad26.COV2.S (Janssen) vaccine were excluded. Participants received their first booster dose 8–9 months after the primary vaccination series, and their second booster 4 to 6 months after the first booster. We report results from blood samples obtained at time points prior to and following the two booster doses. All donor genders were self-reported and informed consent was obtained from all donors.

Cell lines

HEK 293T cells (ATCC) were cultured in DMEM (Corning) containing 10% fetal bovine serum (VWR), and penicillin/streptomycin (Corning) at 37°C/5% CO_2. 293T-ACE2 cells were a gift from Michael Farzan (Scripps Florida) and Nir Hacohen (Broad Institute) and were cultured under the same conditions. Confirmation of ACE2 expression in 293T-ACE2 cells was done via flow cytometry.

METHOD DETAILS

Construction of variant spike expression plasmids

To create variant spike expression plasmids, we performed multiple PCR fragment amplifications utilizing oligonucleotides containing each desired mutation (Integrated DNA Technology) and utilized overlapping fragment assembly to generate the full complement of mutations for each strain. PCR reactions were done with Platinum SuperFI II (Thermofisher) according to the manufacturer's protocol for reaction size and thermocycler protocol. Importantly, we generate these mutations in the context of our previously described

(Garcia-Beltran et al. 2021[56]) codon-optimized SARS-CoV-2 spike expression plasmid harboring a deletion of the C-terminal 18 amino acids that was previously demonstrated to result in higher pseudovirus titers. Assembled fragments were inserted into NotI/XbaI digested pTwist-CMV-BetaGlobin-WPRE-Neo vector utilizing the In-Fusion HD Cloning Kit (Takara) according to the manufacturer's protocol. In-Fusion reactions were transformed into Mix and Go DH5Alpha cells (Zymo Research) according to the manufacturer's protocol and colonies were grown overnight at 37°C to generate plasmid DNA purified using a standard miniprep protocol (Qiagen). All resulting plasmid DNA utilized in the study was verified by whole-plasmid deep sequencing (Illumina or Primordium Labs) to confirm the presence of only the intended mutations and maxi-prepped (Macherey-Nagel) to ensure high quality, high concentrated DNA.

SARS-CoV-2 pseudovirus neutralization assay

To compare the neutralizing activity of vaccinee sera against coronaviruses, we produced lentiviral particles pseudotyped with different spike proteins as previously described (Garcia-Beltran et al. 2021[56]). Briefly, pseudoviruses were produced in 293T cells by PEI transfection of a lentiviral backbone encoding CMV-Luciferase-IRES-ZsGreen as well as lentiviral helper plasmids and each spike variant expression plasmid. Following collection and filtering, production was quantified by titering via flow cytometry on 293T-ACE2 cells. Neutralization assays and readout were performed on a Fluent Automated Workstation (Tecan) liquid handler using 384-well plates (Grenier). 3-fold serial dilutions ranging from 1:12 to 1:8,748 were performed for each serum sample before adding 125–250 infectious units of pseudovirus for 1 h. Subsequently, 293T-ACE2 cells containing polybrene at 8μg/mL were added to each well and incubated at 37°C/5% CO_2 for 48–60 h. Following transduction, cells were lysed using a luciferin-containing buffer[103] and shaken for 5 min prior to quantitation of luciferase expression within 1 h of buffer addition using a Spectramax L luminometer (Molecular Devices) or a Pherastar with Microplate Stacker (BMG Labtech). Percent neutralization was determined by subtracting background luminescence measured in cell control wells (cells only) from sample wells and dividing by virus control wells (virus and cells only). Data was analyzed using Graphpad Prism and pNT_{50} values were calculated by taking the inverse of the 50% inhibitory concentration value for all samples with a neutralization value of 80% or higher at the highest concentration of serum.

Titering

To determine the infectious units of pseudotyped lentiviral vectors, we plated 400,000 293T-ACE2 cells per well of a 12-well plate. 24 h later, three 10-fold serial dilutions of neat pseudovirus supernatant were made in 100 μL of D10, which was then used to replace 100 μL of media on the plated cells. Cells were incubated for 48 h at 37°C/5% CO_2 to allow for expression of ZsGreen reporter gene and harvested with Trypsin-EDTA (Corning). Cells were resuspended in PBS supplemented with 2% FBS (PBS+), fixed with 4% paraformaldehyde (PFA) and analyzed on a Stratedigm S1300Exi Flow Cytometer to determine the percentage of ZsGreen-expressing cells. Infectious units were calculated by determining the percentage of infected cells in wells exhibiting linear decreases in transduction and multiplying by the average number of cells per well determined at the initiation of the assay using FlowJo. At low MOI, (<10% infected cells), each transduced ZsGreen cell was assumed to represent a single infectious unit.

Quantitation of pseudovirus by RT-qPCR

To determine the genome copy concentration of pseudotyped lentiviral vectors, lentiviral RNA was extracted from pseudovirus supernatant using the QIAamp viral RNA mini kit (Qiagen) according to the manufacturer's protocol. Each sample was serially diluted, and each dilution was treated with 1.2 U of Turbo DNase (Invitrogen) at 37°C for 30 min followed by heat inactivation at 75°C for 15 min 10 μL of the treated RNA was used in a 20 μL qRT-PCR reaction with the qScript XLT one-step RT-qPCR Tough Mix, low ROX mix (Quanta Biosciences), a TaqMan probe containing locked nucleic acids (/56-FAM/AGC+C/i5NitInd/GG + GA/ZEN/GCTCTCTGGC/3IABkFQ/) (IDT), and primers designed for targeting the LTR gene of NL4-3 HIV genome, from which the lentiviral vector was derived (5′-GGTCTCTCTIGITAGACCAG and 3′-TTTATTGAGGCTTAAGCAGTGGG) according to the manufacturer's protocol. Each dilution was run in duplicate on a QuantStudio 12K Flex (Applied Biosystems). The following cycling conditions were used: 50°C for 10 min, 95°C for 3 min followed by 50 cycles of 95°C for 15 s and 60°C for 1 min. Virus titer was determined by comparison with a standard curve generated using a plasmid standard generated from serial dilution of CMV-Luciferase-IRES-ZsGreen lentiviral backbone. DNase and No DNase controls were also included at 2.5×10^8 GC/mL of the same plasmid. The range of the assay was from 2.5×10^7 GC/mL to 1.5×10^3 GC/mL. Upon analysis, the average of the three most concentrated dilutions within range of the standard were used to calculate genome copies/mL.

ACE2 spike binding

To determine the ACE2 binding of pseudovirus spike plasmids, each individual spike expression plasmid was co-transfected into 293Ts with a ZSgreen reporter plasmid. Cells were incubated for 48 h at 37°C/5% CO_2 to allow for expression of Spike and ZsGreen reporter genes and harvested with Trypsin-EDTA (Corning). Cells were washed in PBS supplemented with 2% FBS (PBS+), and then stained with Recombinant ACE2 tagged with Alexa Fluor 647 (R&D Systems) at a 1:50 dilution for 30 min in the dark at 4°C. Cells were washed twice with PBS+ and fixed with paraformaldehyde (PFA) for 15 min at 4°C. Finally, cells were washed to remove PFA, resuspended in PBS+ and analyzed on a Stratedigm S1300Exi Flow Cytometer to determine the median fluorescence intensity of ACE2 Alexa Fluor 647 for spike+ (ZSgreen+) cells.

QUANTIFICATION AND STATISTICAL ANALYSIS

Data and statistical analyses were performed using GraphPad Prism 9.0.1, and R v4.0.2. Flow cytometry data was analyzed using FlowJo 10.7.1. For all figures statistical significance was defined by GraphPad Prism as * = $p < 0.0332$, ** = $p < 0.0021$, *** = $p < 0.0002$, **** = $p < 0.0001$. Heatmaps and hierarchical clustering were performed using pheatmap package v1.0.12 in RStudio. The structure used in all figures is PDB ID 6XR8 from https://doi.org/10.1126/science.abd4251 and was chosen given its resolution of the full-length spike allowing us to map all the mutations we made onto the structure. All structures are shown on this PDB to highlight the many mutations from the WT spike and are not meant to represent structures of the variant spikes.